67-6397

SHERWIN, Martin B., 1938-

DYNAMIC BEHAVIOR OF THE WELL STIRRED ISOTHERMAL CRYSTALLIZER.

The City University of New York, Ph.D., 1967
Engineering, chemical

University Microfilms, Inc., Ann Arbor, Michigan

DYNAMIC BEHAVIOR OF THE WELL STIRRED ISOTHERMAL CRYSTALLIZER

by

Martin B. Sherwin

A dissertation submitted to the Graduate Faculty in Engineering in partial fulfillment of the requirements for the degree of Doctor of Philosophy, The City University of New York

1967

This manuscript has been read and accepted for the University Committee in Engineering in satisfaction of the dissertation requirement for the degree of Doctor of Philosophy.

Jan 4 67 — Date

Chairman of Examining Committee

Date

Executive Officer

Prof. R. Graff

Prof. S. Katz

Prof. G. Kranc

Prof. R. Shinnar, Chairman

Supervisory Committee

The City University of New York

Acknowledgment

There are many persons who have contributed, during my education, to the inspiration and motivation required to gain the degree of Doctor of Philosophy. To them I can only say, "Thanks for the encouragement", since it would be improper to mention some and not others.

However, Professor Schmidt, Chairman of the Chemical Engineering Department, is the man who made all this possible and therefore deserves special mention. He helped pioneer the formation of a graduate engineering school and having accomplished this, honored me with a teaching position so I could continue my studies. There is no adequate way for me to express my thanks for these opportunities, but to wish him continued success in his endeavors.

Professor Shinnar and Professor Katz, my primary advisers, made possible the successful completion of this work. Their keen insight into the physics of the problem and familiarity with the tools required for its solution minimized the number of 'impasses' I met, which thus helped to maintain my interest and lead to a rapid conclusion. My contact with these scholars has also matured my general engineering development which is a benefit equally as important as the writing of a thesis.

Thanks are also due to my wife, Beatrice, who took the time from her own studies to type this and other manuscripts and who enjoyed my successes as if they were her own.

I am also appreciative of support from the National Science Foundation for part of this work.

Table of Contents

List of Figures

Abstract

The stability limits and dynamics of the well mixed isothermal crystallizer, with both mixed product and classified product have been studied.

It is shown that for both cases, the primary variable controlling the stability and the dynamics of the system is a sensitivity index called b/g where

$$b/g = \frac{1}{B(\omega)}\frac{dB}{dC} \Big/ \frac{1}{G(\omega)}\frac{dG}{dC}$$

evaluated at the calculated steady state. B is the volumetric rate of nucleation and G is the crystal growth rate.

For the mixed product case with no seeds in the feed the critical value of this parameter above which the system is unstable is 21. Analagously when the product is classified the stability limit is reduced to about 2.5.

Operation in an unstable region results in limit cycles. For the unmixed case the production rate is constant, but the product size and distribution cycle. For the classified case the product size is constant, but the production rate cycles. Both types of behavior will lead to plugging or maloperation of the associated filters or centrifuges.

Discussions of the internal feedback mechanism causing this behavior point out possibilities for damping these limit cycles, which are not today used in industry.

Introduction

Industrial crystallization operations are still something of an art, and often depend to a considerable degree on the skill of the operator. This paper attempts to aid in the understanding of the dynamic behavior and stability of such systems.

The special feature which distinguishes continuous crystallization processes from other continuous reactors is the simultaneous occurence of nucleation and growth. Both of these steps depend on supersaturation as a driving force, with the rate dependence of nucleation on supersaturation being highly non linear. In a well mixed crystallizer these steps occur simultaneously and homogeneously throughout the vessel.

It has been observed that continuous crystallization processes are under some conditions inherently unstable and of a cyclic nature (9,10). Randolph and Larson (11) speculated that the instability and long-term transients in the size distribution observed in an ammonium sulfate crystallizer were due to changes in operation over a three shift period rather than inherent to the system. Saeman (9) found that it was impossible to operate a completely classified ammonium nitrate crystallizer continuously, but was forced to periodically discharge product in a cyclic manner. Changing the operation to a well mixed crystallizer alleviated, but did not not completely remove the operating problems.

The author, during a plant start-up, found it impossible to operate a well stirred isothermal fumaric acid crystallizer in a continuous manner, but experienced considerable cycling of the product size. Much of this unsteady behavior occurs despite the fact that heat and material inputs and other operating conditions are held constant. Similar observations have been made in some continuous polymerization and fermentation processes which also involve nucleation and growth (5, 16).

Theoretical papers dealing with industrial crystallization are very few in number and deal mainly with steady-state behavior (2, 13). Experimental and theoretical studies on nucleation or growth usually focus on just one of these kinetic steps, thereby avoiding the problem of interaction. This study of the dynamics of the well stirred crystallizer considers these interactions and tries to analyze what effect variation in operation will have on them. An explanation is proposed for the observed difficulty of attaining continuous stable operation in some cases and means of correcting this behavior become apparent from the text.

Though considerable effort has been spent on the study of the dynamical behavior of both homogeneous and heterogeneous reaction systems (1, 3, 19), very few studies deal with the effect of nucleation. Part of this is due to the extreme difficulty in the mathematical treatment of such

systems in all but the most simple cases.

Larson (11) has made a theoretical linearized stability analysis of a completely mixed crystallizer, and found that under most practical conditions it should be stable. But in an experimental step response study of one typical crystallization the same author also found strong tendency toward long term cyclic transients.

Larson's analysis contains some very strong simplifications, particularly in the neglect of a metastable region of low nucleation rate. It is just this strong non linear dependence of nucleation rate on supersaturation that causes the observed cyclic changes in particle size. Our linearized stability analysis allows for such effects, and hence shows both regions of stable and unstable operation.

A linearized stability analysis will only indicate if the system is stable or not, and not give any indication as to the magnitude of the fluctuations. Fortunately, for a mixed vessel it is in many cases possible to follow the behavior of a disturbance in the non linear region and to compute the amplitude of the fluctuations.

The approach used in this work was presented in a recent paper by Katz and Hulburt (7) which allowed a reasonably realistic, theoretical treatment for quite complex situations.

3. Non Classified Product

3.1 Derivation of the model

A diagram of the type of operation discussed is shown below:

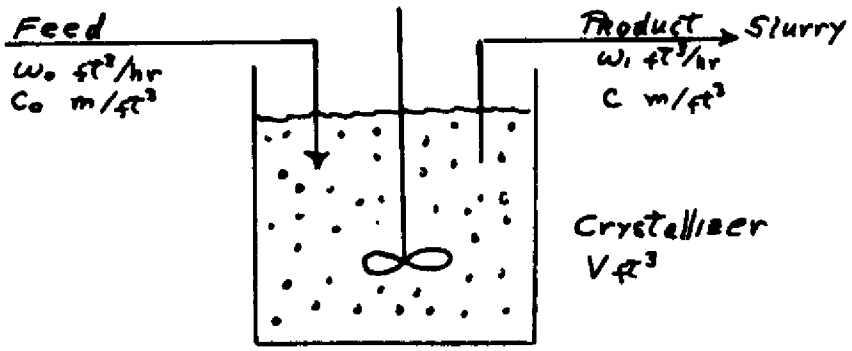

A feed material containing solute at concentration C_o is fed to a crystallizer at a volumetric rate ω_o. The crystallizer is well mixed and isothermal so that instant cooling of the feed results in a supersaturation driving force for subsequent nucleation and growth. A product slurry is withdrawn at volumetric rate ω_1.

The equations describing the behavior of this system are derived in the following section:

In order to describe the behaviour of the Isothermal Mixed Suspension Mixed Product Removal Crystallizer, balances must be written for the particles and the crystallizing material. In addition to these general balances, appropriate kinetic relations must be added for the description to be complete.

In writing these balances, the following assumptions

were made:

The crystal particles are assumed to be regular solids which maintain their shape upon growth and can therefore be characterized geometrically by a linear dimension r.

For solids which grow in three dimensions, the volume of any crystal is given by kr^3, where k is the appropriate geometrical shape factor. (This paper will deal with the case of a three dimensional crystal since it is the most common, although the assumption of plate or needle shaped crystals, which grow in two and one dimensions respectively, could just as easily be substituted).

The crystal density ρ is taken to be constant.

The particle size distribution is the number density f, at size r, such that

$f(r,t)dr$ = the number of crystals per unit volume of crystallizer having radii in the range r, r + dr at time t.

The fractional volume ε, occupied by the solution is a function of time and can be defined in terms of f

$$1 - \varepsilon(t) = \int_0^\infty k r^3 f(r,t)\,dr \qquad (1)$$

Similarly, when a seeded feed is used.

$\psi(r,t)dr$ = the number of crystals per unit volume of feed having radii in the range r, r + dr at time t.

and the fractional volume ε_0, occupied by the feed solution is

$$1-\varepsilon_0(t)=\int_0^\infty \kappa r^3 \psi(r,t)\,dr \qquad (2)$$

The growth rate of an existing crystal dr/dt is assumed to be described by the product of a function of crystal environment G (c) and a function of crystal size $\phi(r)$ such that

$$\frac{dr}{dt}=G(c)\,\phi(r) \qquad (3)$$

where c is the solute concentration per volume of solution.

The nucleation rate for new crystals is mainly a function of solute concentration in the crystallizer according to the classical theories of Volmer (17) and Mier (18). It is assumed that the size distribution of new crystals appears as a Dirac delta function, or that all new crystals are formed at a nominal size r_0.

B (c) = number of crystals born per volume of solution per unit time at r_0 .

ω_0 and ω_1 are the volumetric feed and withdrawal rates to and from the crystallizer working volume V.

3.11 Conservation Equations

Now the appropriate balances over the crystallizer can be written down. (A detailed derivation of the particle balance can be found in reference 5.)

Particle Balance

$$\frac{\partial[Vf]}{\partial t}+\frac{\partial[G\phi Vf]}{\partial r}=\varepsilon V B\,\delta(r-r_0)-\omega_1 f+\omega_0 \psi \qquad (4)$$

Solute and Crystal Balance

$$\frac{d}{dt}[V(\varepsilon C+(1-\varepsilon)\rho)]=\omega_0[\varepsilon_0 C_0+(1-\varepsilon_0)\rho]-\omega_1[\varepsilon C+(1-\varepsilon)\rho] \qquad (5)$$

When equation (4) is multiplied by kr^3 and integrated over r, the following relation is obtained:

$$\frac{d}{dt}[(1-\varepsilon)V] = GV\sigma + \varepsilon VBKr_0^3 + \omega_0(1-\varepsilon_0) - \omega_1(1-\varepsilon) \tag{6}$$

where

$$\sigma = 3K\int_0^\infty r^2 f \phi\, dr \tag{7}$$

If a balance were written for the solvent and this relation combined with (5) and (6), one could obtain an expression for the variation of the working volume V, with time. The resulting expression is:

$$\frac{dV}{dt} = (\omega_0-\omega_1) + (1-\bar{\nu}\rho)(\sigma VG + \varepsilon VBKr_0^3) \tag{8}$$

where $\bar{\nu}$ is the partial molar volume of the solute. Available data indicate that taking $\bar{\nu} = \frac{1}{\rho}$ is quite a reasonable assumption, so that if we specify that $\omega_0 = \omega_1 = \omega$, the working volume remains constant.

It is desirable to have a relation expressing the variation of solute concentration c with time, since both G and B are expressed in terms of this variable. Equations (5) and (6) can be used along with the assumption of constant volume to yield the desired expression:

$$\varepsilon\frac{dc}{dt} = \frac{\omega}{V}(c_0-c)\varepsilon_0 - (\rho-c)(\sigma G + \varepsilon BKr_0^3) \tag{9}$$

The working set of equations is now:

$$\frac{\partial f}{\partial t} + \frac{\partial}{\partial r}[G\phi f] = \varepsilon B\delta(r-r_0) + \frac{\omega}{V}\psi - \frac{\omega}{V}f \tag{10}$$

$$\varepsilon \frac{dc}{dt} = \frac{\omega}{V}(c_0 - c)\varepsilon_0 - (\rho - c)(\sigma G + \varepsilon B K r_0^3) \tag{11}$$

where $\sigma = 3K\int_0^\infty r^2 f \phi \, dr$

3.12 Moment Equations

The above set of equations is difficult to solve, even numerically, since it contains a partial differential equation for f(r, t). If it is not necessary to determine how the distribution f varies with time, but a knowledge of the variation of its moments with time is satisfactory, the set can be transformed to a group of ordinary differential equations. The 'nth' moment of f will be called μ_n while the expressions in pointed brackets are averages over f in the same sense; in general

$$\langle \eta \rangle = \int_0^\infty \eta f \, dr \tag{12}$$

$$\mu_n(t) = \int_0^\infty r^n f(r,t) \, dr \tag{13}$$

The physical significance of the moments of f is shown below:

$\mu_0 = \int_0^\infty f \, dr$ = total number of crystals per unit volume of crystallizer

$\mu_1 = \int_0^\infty r f \, dr$ = total 'radius' of crystals per unit volume of crystallizer

$3K\mu_2 = 3K\int_0^\infty r^2 f \, dr$ = total surface of crystals per unit volume of crystallizer

$K\mu_3 = K\int_0^\infty r^3 f \, dr \cdot (1-\varepsilon)$ = volume fraction of solids

In the same manner, the moments of the seed crystal distribution can be written:

$$\mu_n(t) = \int_0^\infty r^n \psi(r,t)\, dr \tag{14}$$

and these moments retain the same physical significance as the corresponding moments related to f per unit volume of feed.

The weight distribution of the crystals W (r) can be written:

$$W(r) = \rho K r^3 f(r) \tag{15}$$

so that the mean particle size with respect to the weight distribution is:

$$\text{Mean Particle Size} = r_{wm} = \frac{\int_0^\infty r W(r)\, dr}{\int_0^\infty W(r)\, dr} = \frac{\rho K \int_0^\infty r^4 f(r)\, dr}{\rho K \int_0^\infty r^3 f(r)\, dr} = \frac{\mu_4}{\mu_3} \tag{16}$$

The Variance of the weight distribution is:

$$\text{Variance} = \frac{\int_0^\infty (r - r_{wm})^2 W(r)\, dr}{\int_0^\infty W(r)\, dr} = \frac{\int_0^\infty r^2 W(r)\, dr - 2 r_{wm} \int_0^\infty W(r)\, dr + r_{wm}^2 \int_0^\infty W(r)\, dr}{\int_0^\infty W(r)\, dr} \tag{17}$$

which, in terms of the number distribution, is:

$$\text{Variance} = \frac{\mu_5}{\mu_3} - \left(\frac{\mu_4}{\mu_3}\right)^2 \tag{18}$$

The Coefficient of Variation γ of the weight distribution is a measure of its uniformity.

$$\gamma^2 = \frac{\text{Variance}}{(\text{Mean Size})^2} = \frac{\frac{\mu_5}{\mu_3} - \left(\frac{\mu_4}{\mu_3}\right)^2}{\left(\frac{\mu_4}{\mu_3}\right)^2} \tag{19}$$

Clearly all these moments can be determined by a microscopic analysis or a sieve analysis of the crystallizer product. It is also clear that a knowledge of these moments is enough to characterize the performance of a crystallizer.

By multiplying equation (10) through by r^n and integrating, the moment equations can be generated.

$$\frac{d\mu_n}{dt} = nG(t)\langle r^{n-1}\phi(r)\rangle + \mathcal{E}B(t)r_0^n + \frac{\omega}{V}\gamma_n - \frac{\omega}{V}\mu_n \qquad n=0,1,2,3\ldots \tag{20}$$

where

$$\langle r^{n-1}\phi(r)\rangle = \int_0^\infty r^{n-1}\phi(r)f\,dr \tag{21}$$

Now the series of equations (20) plus equation (11) are the set of equations describing the system. These, however, do not necessarily give a self-contained set of equations because of the dependence of particle growth on r, as manifested in the terms $\langle r^{n-1}\phi\rangle$. If dr/dt is independent of r, then $\phi = 1$ and $\langle r^{n-1}\phi\rangle$ is simply μ_{n-1} and the equations close satisfactorily at n = 3. This is so even if dr/dt depends linearly on r, but more awkward terms of dependence (r^2, r^3, etc.,) can only be handled by making successive approximations to f (r, t) in the term of Laguerre series as discussed in reference (7).

Fortunately, a number of investigators (8, 12, 15) have found that, in many cases, the growth rate does not depend on r to any significant amount, so that in the following sections it is assumed that $\phi = 1$.

Later in the paper, growth models of the form

$$\frac{dr}{dt} = G(t)[1+ar]$$

which include a size dependent term will be studied to illustrate the effect of this dependence.

Remembering that $I-\varepsilon = \int_0^\infty Kr^3 f\,dr$ we get the following closed set of equations:

$$\frac{d\mu_0}{dt} = (1-K\mu_3)B(t) - \frac{w}{V}\mu_0 + \frac{w}{V}\eta_0$$

$$\frac{d\mu_1}{dt} = G(t)\mu_0 + (1-K\mu_3)B(t)r_0 - \frac{w}{V}\mu_1 + \frac{w}{V}\eta_1$$

$$\frac{d\mu_2}{dt} = 2G(t)\mu_1 + (1-K\mu_3)B(t)r_0^2 - \frac{w}{V}\mu_2 + \frac{w}{V}\eta_2 \qquad (22)$$

$$\frac{d\mu_3}{dt} = 3G(t)\mu_2 + (1-K\mu_3)B(t)r_0^3 - \frac{w}{V}\mu_3 + \frac{w}{V}\eta_3$$

$$(1-K\mu_3)\frac{dc}{dt} = \frac{w}{V}(c_0-c)\varepsilon_0 - (\rho-c)(3G(t)K\mu_2 + (1-K\mu_3)B(t)Kr_0^3)$$

In order to solve this set of equations to trace

the history of c(t) and the moments of f(r, t), the system (22) must be supplemented by the initial conditions and the feed rate and composition as a function of time. Also the dependence of B(c) and G(c) on concentration c(t) must be specified.

3.13 Steady State Equations

In order to get the steady state moments, the particle distribution f must first be obtained. This can be used to generate the moment relations.

The steady state particle balance can be written down from (10), remembering that we are now assuming $\phi = 1.0$.

$$\bar{G}\omega \frac{d\bar{f}}{dr} = \bar{\varepsilon}\bar{B}\omega\,\delta(r-r_0) - \frac{\bar{\omega}}{V}\bar{f}(r) + \frac{\bar{\omega}}{V}\bar{\psi}(r) \tag{23}$$

where the superscript bars indicate steady state values.

This can be solved, giving:

$$\bar{f} = \frac{\bar{\varepsilon}\bar{B}}{\bar{G}}\, e^{-\frac{\bar{\omega}}{V\bar{G}}(r-r_0)} + \frac{\bar{\omega}}{V\bar{G}}\int_0^r \psi(x)\, e^{-\frac{\bar{\omega}}{V\bar{G}}(r-x)}\,dx \tag{24}$$

The moments can now be obtained by straightforward calculation from (24).

$$\bar{\mu}_0 = \frac{\bar{\varepsilon}\bar{B}}{\bar{G}}\left(\frac{V\bar{G}}{\bar{\omega}}\right) + \gamma_0$$

$$\bar{\mu}_1 = \frac{\bar{\varepsilon}\bar{B}}{\bar{G}}\left(\frac{V\bar{G}}{\bar{\omega}}\right)^2\left[\left(\frac{\bar{\omega}}{V\bar{G}}r_0\right)+1\right] + \frac{V\bar{G}}{\bar{\omega}}\gamma_0 + \gamma_1$$

$$\bar{\mu}_2 = \frac{\bar{\varepsilon}\bar{B}}{\bar{G}}\left(\frac{V\bar{G}}{\bar{\omega}}\right)^3\left[\left(\frac{\bar{\omega}}{V\bar{G}}r_0\right)^2 + 2\left(\frac{\bar{\omega}}{V\bar{G}}r_0\right)+2\right] + 2\left(\frac{V\bar{G}}{\bar{\omega}}\right)^2\gamma_0 + 2\left(\frac{V\bar{G}}{\bar{\omega}}\right)\gamma_1 + \gamma_2$$

$$\bar{\mu}_3 = \frac{\bar{\varepsilon}\bar{B}}{\bar{G}}\left(\frac{V\bar{G}}{\omega}\right)^4\left[\left(\frac{\omega}{V\bar{G}}r_0\right)^3 + 3\left(\frac{\omega}{V\bar{G}}r_0\right)^2 + 6\left(\frac{\omega}{V\bar{G}}r_0\right) + 6\right]$$
$$+ 6\left(\frac{V\bar{G}}{\omega}\right)^3\gamma_0 + 6\left(\frac{V\bar{G}}{\omega}\right)\gamma_1 + 3\left(\frac{V\bar{G}}{\omega}\right)\gamma_2 + \gamma_3$$

$$\bar{\mu}_4 = \frac{\bar{\varepsilon}\bar{B}}{\bar{G}}\left(\frac{V\bar{G}}{\omega}\right)^5\left[\left(\frac{\omega}{V\bar{G}}r_0\right)^4 + 4\left(\frac{\omega}{V\bar{G}}r_0\right)^3 + 12\left(\frac{\omega}{V\bar{G}}r_0\right)^2 + 24\left(\frac{\omega}{V\bar{G}}r_0\right) + 24\right]$$
$$+ 24\left(\frac{V\bar{G}}{\omega}\right)^4\gamma_0 + 24\left(\frac{V\bar{G}}{\omega}\right)^3\gamma_1 + 12\left(\frac{V\bar{G}}{\omega}\right)^2\gamma_2 + 4\left(\frac{V\bar{G}}{\omega}\right)\gamma_3 + \gamma_4 \qquad (25)$$

$$\bar{\mu}_5 = \frac{\bar{\varepsilon}\bar{B}}{\bar{G}}\left(\frac{V\bar{G}}{\omega}\right)^6\left[\left(\frac{\omega}{V\bar{G}}r_0\right)^5 + 5\left(\frac{\omega}{V\bar{G}}r_0\right)^4 + 20\left(\frac{\omega}{V\bar{G}}r_0\right)^3 + 60\left(\frac{\omega}{V\bar{G}}r_0\right)^2 + 120\left(\frac{\omega}{V\bar{G}}r_0\right) + 120\right]$$
$$+ 120\left(\frac{V\bar{G}}{\omega}\right)^5\gamma_0 + 120\left(\frac{V\bar{G}}{\omega}\right)^4\gamma_1 + 60\left(\frac{V\bar{G}}{\omega}\right)^3\gamma_2 + 20\left(\frac{V\bar{G}}{\omega}\right)^2\gamma_3 + 5\left(\frac{V\bar{G}}{\omega}\right)\gamma_4 + \gamma_5$$

An additional relation which will be of use later is derived from the last two relations in set (22).

$$\bar{\varepsilon} = 1 - K\bar{\mu}_3 = \left(\frac{\rho - \zeta_0}{\rho - \bar{\zeta}}\right)\bar{\varepsilon}_0 \qquad (26)$$

3.2 Linearization of the Model

In order to determine under what conditions instability in the system will occur, the set of equations describing the system (22) must be linearized about the steady state. Then the conditions under which a small displacement from the steady state will grow may be determined via the conventional use of the Routh-Horwitz criteria.

Primed quantities indicate the departure from the steady state values (superscript bar).

The feed rate and concentration can vary in time in the form:

$$\omega(t) = \bar{\omega} + \omega'(t) \tag{27}$$

$$C_o(t) = \bar{C}_o + C_o'(t)$$

The initial conditions are:

$$C(0) = \bar{C} \tag{28}$$

$$\mu_n(0) = \bar{\mu}_n \qquad n = 0,1,2,3\ldots$$

The performance variables are represented by:

$$\mu_n(t) = \bar{\mu}_n + \mu_n'(t) \qquad n = 0,1,2,3\ldots \tag{29}$$

$$C(t) = \bar{C} + C'(t)$$

The kinetic terms for small displacements can be written:

$$B(c,t) = \bar{B}(\bar{c}) + \frac{dB}{dC}(\bar{c}) \cdot C' \tag{30}$$

$$G(c,t) = \bar{G}(\bar{c}) + \frac{dG}{dC}(\bar{c}) \cdot C'$$

In addition, the following dimensionless variables are defined:

$$q = \frac{\bar{\varepsilon}_o(1-\bar{\varepsilon})(\bar{C}_o-\bar{C})}{\bar{\varepsilon}(\bar{\varepsilon}_o-\bar{\varepsilon})\bar{G}}\frac{dG(\bar{c})}{dC} \tag{31}$$

$$b = \frac{\bar{\varepsilon}_o(1-\bar{\varepsilon})(\bar{C}_o-\bar{C})}{\bar{\varepsilon}(\bar{\varepsilon}_o-\bar{\varepsilon})\bar{B}}\frac{dB(\bar{c})}{dC} \tag{32}$$

where

$$\bar{\varepsilon} = 1-\kappa\bar{\mu}_3$$

$$\bar{\varepsilon}_o = 1-\kappa\bar{\eta}_3$$

$$Z_n' = \frac{\mu_n'}{\mu_n} \qquad n=0,1,2,3,\ldots \tag{33}$$

$$Y' = \frac{\bar{\varepsilon}(\bar{\varepsilon}_o-\bar{\varepsilon})}{\bar{\varepsilon}_o(1-\bar{\varepsilon})}\frac{C'}{\bar{C}_o-\bar{C}}$$

$$\theta = t(\bar{\omega}/V)$$

$$\rho(\theta) = \omega'(\theta)/\bar{\omega}$$

$$g(\theta) = \frac{\bar{C}_o-\bar{\varepsilon}}{1-\bar{\varepsilon}}\frac{C_o'(\theta)}{\bar{C}_o-\bar{C}}$$

Now, substituting (27-33) into (22) and utilizing the steady state relations results in the following set:

$$\frac{dZ_n'}{d\theta} - \left[\left(n\frac{\bar{\mu}_{n-1}}{\bar{\mu}_n}\frac{V\bar{G}}{\bar{\omega}}\right)q + \left(1-\frac{\bar{\eta}_n}{\bar{\mu}_n}\right)b - \left(n\frac{\bar{\mu}_{n-1}}{\bar{\mu}_n}\frac{V\bar{G}}{\bar{\omega}}\right)b\right]Y'$$

$$-\left[n\frac{\bar{\mu}_{n-1}}{\bar{\mu}_n}\frac{V\bar{G}}{\bar{\omega}}\right]Z_{n-1}' + \left[\kappa r_o^n\bar{B}\frac{V}{\bar{\omega}}\frac{\bar{\mu}_3}{\bar{\mu}_n}\right]Z_3' + Z_n' \tag{34}$$

$$= -\rho(\theta)\left[1-\frac{\bar{\eta}_n}{\bar{\mu}_n}\right] \qquad n=0,1,2,3\ldots$$

$$\frac{dY'}{d\theta} + \left[\left(3\frac{\bar{\mu}_2}{\bar{\mu}_3}\frac{V\bar{G}}{\bar{\omega}}\right)g + \left(1-\frac{\bar{\gamma}_3}{\bar{\mu}_3}\right)b - \left(3\frac{\bar{\mu}_2}{\bar{\mu}_3}\frac{V\bar{G}}{\bar{\omega}}\right)b\right]Y' + Y'$$

$$+ \left[3\frac{\bar{\mu}_2}{\bar{\mu}_3}\frac{V\bar{G}}{\bar{\omega}}\right]Z_2' - \left[Kr_0^3\bar{B}\frac{V}{\bar{\omega}}\right]Z_3' = g(\theta) + \left[1-\frac{\bar{\gamma}_3}{\bar{\mu}_3}\right]p(\theta)$$

There are three sets of dimensionless groups containing steady state variables which arise in (34):

$$L_n = n\,\frac{\bar{\mu}_{n-1}}{\bar{\mu}_n}\,\frac{V\bar{G}}{\bar{\omega}} \qquad n=0,1,2,3\ldots \tag{35}$$

$$R_n = Kr_0^3\bar{B}\frac{V}{\bar{\omega}}\,\frac{\bar{\mu}_3}{\bar{\mu}_n} \qquad n=0,1,2,3\ldots \tag{36}$$

$$S_n = \frac{\bar{\gamma}_n}{\bar{\mu}_n} \qquad n=0,1,2,3\ldots \tag{37}$$

besides the dimensionless kinetic parameters b and g which have been defined in equations (31) and (32).

These sets of dimensionless groups Ln, Rn, and Sn depend on a finite number of steady state parameters contained in equation (25). The identification and dependence of the model on these parameters will be discussed in succeeding sections.

3.3 Kinetic Models

Some well known growth and nucleation models are now briefly introduced and substituted into equations (31) and (32) in order to relate these important dimensionless kinetic parameters to the physical variables of the system.

It should be mentioned here that the later sections will show that the ratio of these two groups, b/g, is of primary importance in determining the stability and dynamic behavio r of the model.

3.31 Growth Model

Many investigators have found the relation between G and c to be satisfied by

$$G(c) = K_1 (C - C_s) \tag{38}$$

where k_1 is a constant for isothermal operation and c_s is the solubility concentration of the solute. Substituting this model into equation (31) yields

$$g = \frac{\bar{\varepsilon}_o(1-\bar{\varepsilon})}{\bar{\varepsilon}(\bar{\varepsilon}_o-\bar{\varepsilon})} \; \frac{\bar{C}_o-\bar{C}}{\bar{C}-C_s} \tag{39}$$

Generally, the supersaturation ($c-c_s$) of crystallizing systems is quite small when compared to the difference between feed and outlet concentrations, so that normally the value of g should be of the order of magnitude 10^2-to 10^3.

3.32 Nucleation Models

Volmer's model (15, 17) is based on thermodynamic

considerations and gives rise to an Arrhenius type function.

$$B(\sigma) = K_2 \, C \, e^{\frac{-K_3}{[\ln \frac{C}{C_s}]^2}} \tag{40}$$

Substituting this model in equation (32) yields:

$$b = \frac{\bar{\varepsilon}_o(1-\bar{\varepsilon})}{\bar{\varepsilon}(\bar{\varepsilon}_o-\bar{\varepsilon})} \frac{2K_3(\bar{C}_o-\bar{C})}{\bar{C}[\ln \frac{C}{C_s}]^2} \approx \frac{\bar{\varepsilon}_o(1-\bar{\varepsilon})}{\bar{\varepsilon}(\bar{\varepsilon}_o-\bar{\varepsilon})} \frac{2K_3}{\bar{C}(\frac{\bar{C}}{C_s}-1)^3} \tag{41}$$

the latter approximation being made since $(\frac{\bar{C}}{C_s} - 1)$ is very small for crystallization systems.

Then using the kinetic models given by equations (38) and (40), the term b/g can be approximated by:

$$\frac{b}{g} \approx \frac{2K_3(\bar{C}-C_s)}{(\frac{\bar{C}}{C_s}-1)^3 \bar{C}} = \frac{2K_3 C_s}{(\frac{\bar{C}}{C_s}-1)^2 \bar{C}} \approx \frac{2K_3}{(\frac{C}{C_s}-1)^2} \tag{42}$$

The term b/g represents the sensitivity ratio of the nucleation to growth functions at steady state conditions and it can be seen that,as the solute concentration approaches its solubility limit, this term rapidly increases in value. This means that as one tries to grow larger crystals, a critical size should be reached where the stability limits are exceeded.

Another nucleation model which is a simplified representation of equation (40) is Mier's metastable model (18) which can be written:

$$B = K_4(C-C_M)^m \qquad C > C_M$$
$$B = 0 \qquad C \leq C_M \tag{43}$$

where k_4 is a constant, C_M is the metastable concentration, above which nucleation occurs and m is some power. Combining this with equation (38) we get:

$$\frac{b}{g} = m\,\frac{\bar{C}-C_s}{\bar{C}-C_M} \qquad C>C_M \tag{44}$$

Here it is evident that as the solute concentration approaches the metastable limit C_M from above, the sensitivity ratio b/g will increase in value.

3.4 Stability Analysis

3.41 Clear Feed

The simplification of a clear feed, such that $\mathcal{E}_o = 1.0$ imposed here. Many crystallizers operate in this manner since it alleviates the problem of preparing and metering seed nuclei into the system.

This assumption means the following:

$$\psi = 0.$$

$$\gamma_n = 0. \qquad n = 0, 1, 2, 3 \ldots$$

$$\mathcal{E}_o = 1.0$$

which considerably simplifies the relations previously derived.

The dimensionless groups arising in the set of linearized equations (34) reduce to two, Ln and Rn as defined in equations (35) and (36) since the Sn are zero for the clear feed case. Before substituting the steady state relations (25) into (35) and (36) to determine Ln and Rn, we define a new group:

$$\alpha = \left(\frac{\bar{\omega}}{v\bar{G}} r_o \right) \tag{45}$$

This group is the ratio of the nuclei radius divided by the steady state growth, per draw-down time .

Now substituting (25) and (45) into (35) and (36), we get:

$$L_0 = 0$$

$$L_1 = \frac{1.}{\alpha + 1.}$$

$$L_2 = \frac{2\,[\alpha+1.]}{[\alpha^2+2\alpha+2]} \tag{46}$$

$$L_3 = \frac{3\,[\alpha^2+2\alpha+2]}{[\alpha^3+3\alpha^2+6\alpha+6]}$$

$$R_0 = \frac{(1-\bar{\varepsilon})}{\bar{\varepsilon}}$$

$$R_1 = \frac{(1-\bar{\varepsilon})}{\bar{\varepsilon}} \frac{\alpha}{\alpha+1} \tag{47}$$

$$R_2 = \frac{(1-\bar{\varepsilon})}{\bar{\varepsilon}} \frac{\alpha^2}{\alpha^2+2\alpha+2}$$

$$R_3 = \frac{(1-\bar{\varepsilon})}{\bar{\varepsilon}} \frac{\alpha^3}{\alpha^3+3\alpha^2+6\alpha+6}$$

The groups Ln are functions of α only while Rn are function of both α and $\bar{\varepsilon}$. Values of Ln and Rn for the fourth and fifth moments can also be found without difficulty, when needed.

The closed set of linearized equations can now be written as follows:

$$\frac{dz_0'}{d\theta} + z_0' + R_0 z_3' - b\,y' = -p(\theta)$$

$$\frac{dz_1'}{d\theta} - L_1 z_0' + z_1' + R_1 z_3' - [L_1 g + (1-L_1)b]\,y' = -p(\theta)$$

$$\frac{dz_2'}{d\theta} - L_2 z_1' + z_2' + R_2 z_3' - [L_2 g + (1-L_2)b]\,y' = -p(\theta) \qquad (48)$$

$$\frac{dz_3'}{d\theta} - L_3 z_2' + [1+R_3] z_3' - [L_3 g + (1-L_3)b]\,y' = -p(\theta)$$

$$\frac{dy'}{d\theta} + L_3 z_2' - R_3 z_3' + [L_3 g + (1-L_3)b + 1]\,y' = p(\theta) + g(\theta)$$

The eigenvalues of this set of equations can be found directly or the set of linear differential equations can be reduced to a set of algebraic equations by taking the LaPlace transforms. In the latter case, the location of the poles of the transfer function would determine the stability of the system.

α, $\bar{\epsilon}$, b and g are the parameters of the system which determine the location of the poles of the transfer function. The results of applying the Routh-Horwitz criteria to this set of equations are presented in Figures 1 and 2 (See Appendix 6.1). It is very surprising (Fig. 1) that $\bar{\epsilon}$ has such a negligible effect on the limits of stable operation.

It was found that for small values of α (which is

FIGURE 1
STABILITY LIMITS AS A FUNCTION OF LIQUID VOLUME FRACTION ε ($\alpha = 0.1$)

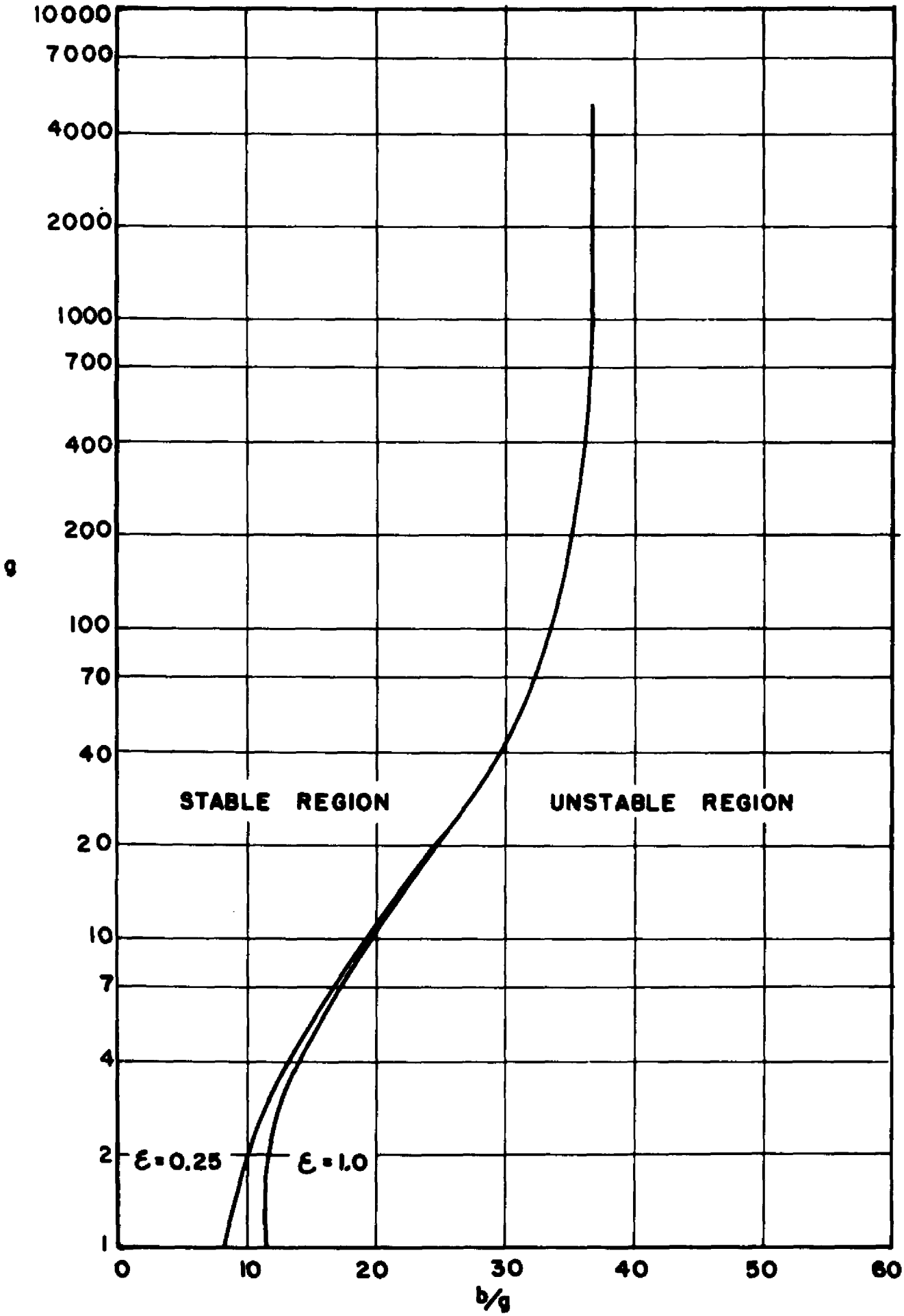

FIGURE 2
STABILITY LIMITS AS A FUNCTION OF NUCLEI SIZE PARAMETER α ($\varepsilon = 0.8$)

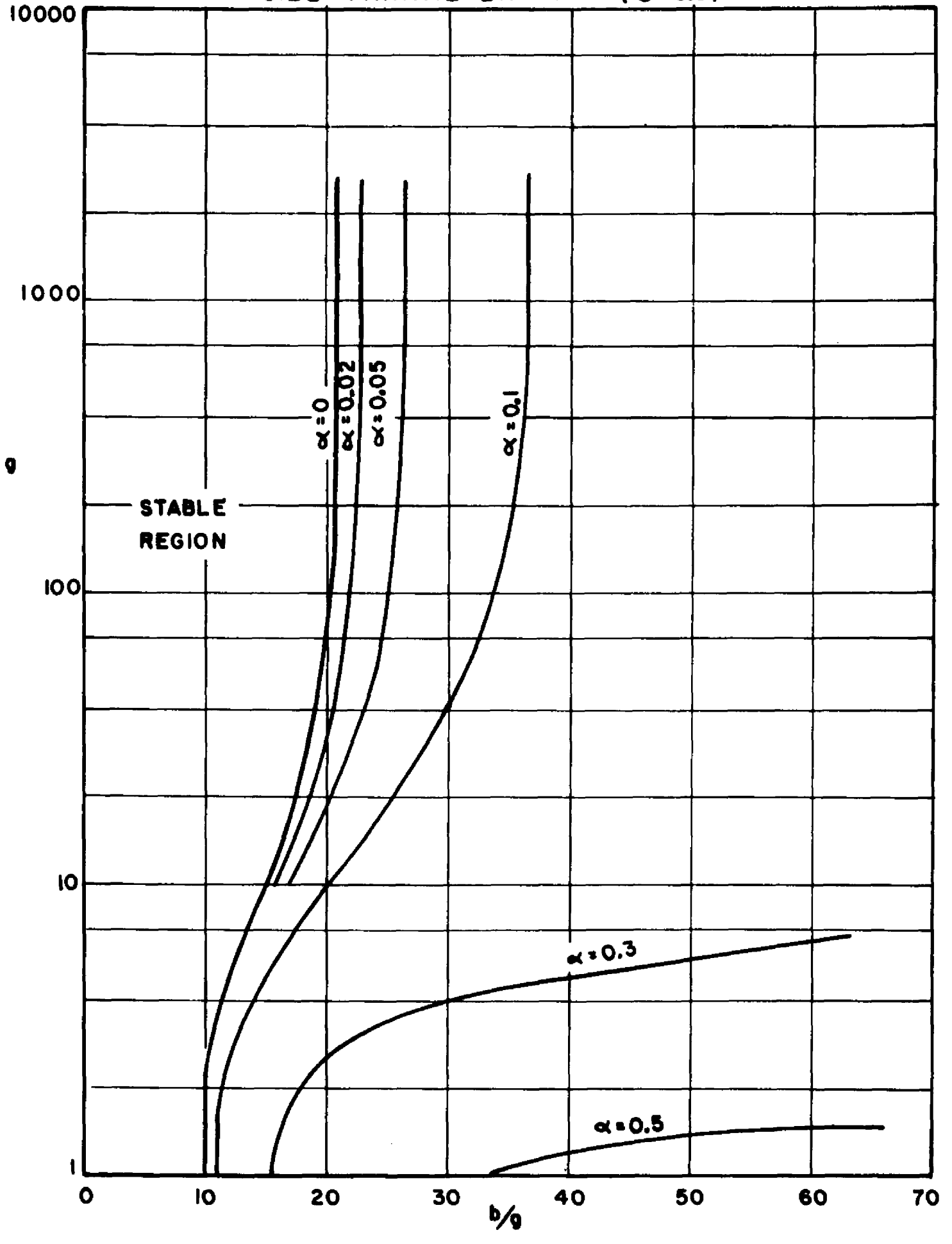

FIGURE 3

LIMITING VALUES OF b/g vs. α

$(0 \leq \alpha \leq 0.1)$

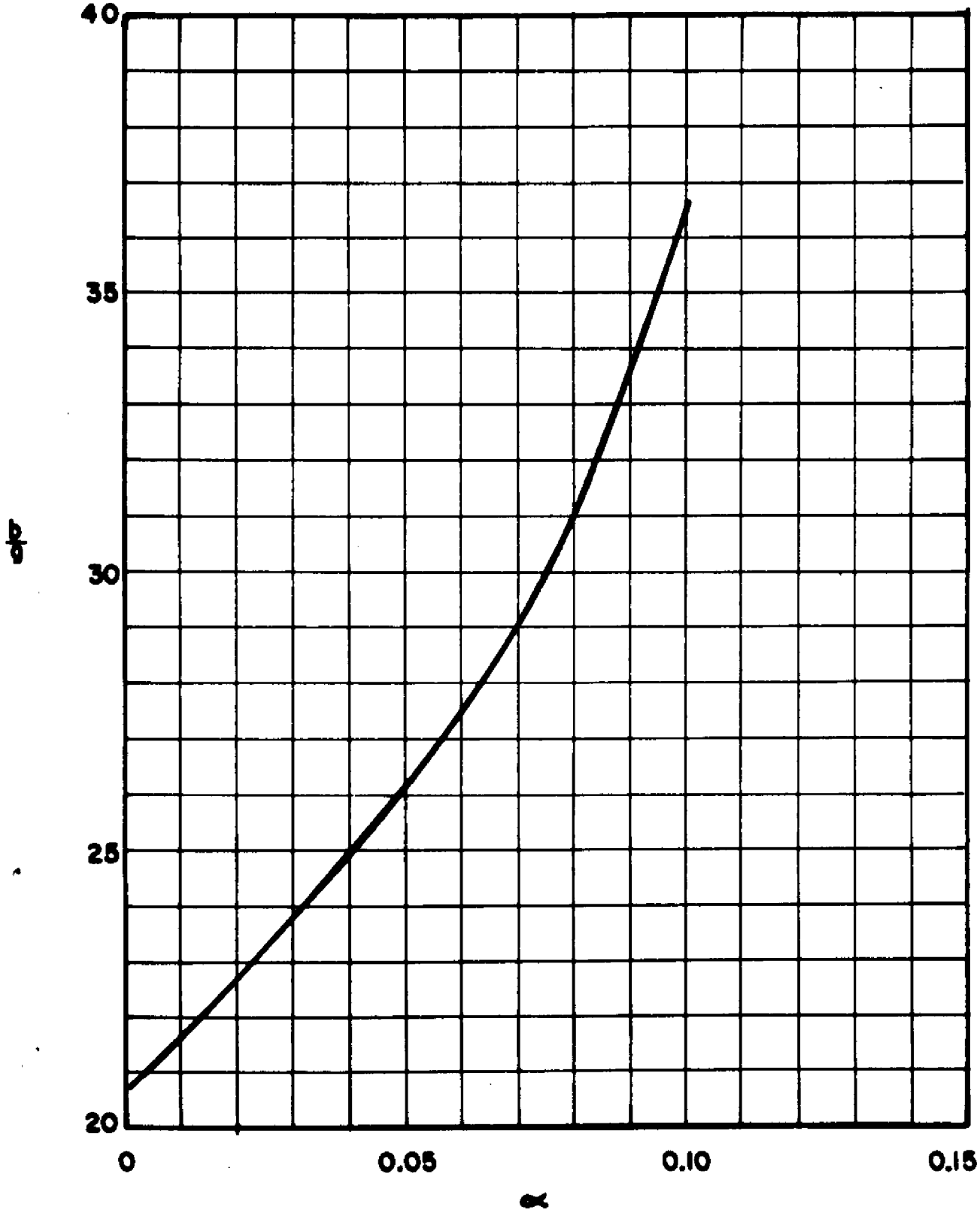

most pertinent to crystallization), the ratio of b/g reached a limiting value with increasing values of g. For this reason the attached Figures indicate g and b/g as the system parameters, rather than g and b. For high values of g, the stability depends on the single parameter b/g (critical) which is a unique function of α or the ratio of nuclei size to the average linear size increase of a crystal per draw-down time (Fig. 3).

For most crystallization systems α will have values close to zero and in the past, investigators (2, 11, 13) have taken α equal to zero.

3.42 Effect of Seed Addition

For the special case when the seed size is identical to the generated nuclei size (both distributions appearing as delta functions) the results of the preceeding section can be used to predict the effect of seed addition on the system's stability. The nucleation term B(c) is expanded to include all nuclei entering the system as shown below:

$$B(c)_{\text{Total}} = B(c)_{\text{nucleated}} + \frac{\psi}{\varepsilon}\frac{\bar{\omega}}{V} \qquad (49)$$

where ψ is defined to be the number of seeds per unit volume of feed so that $\frac{\psi\bar{\omega}}{\varepsilon V}$ is the seed addition rate per unit volume of crystallizer solution.

If we represent the steady state number of seeds as equals to ζ time the generated nuclei (superscript bar indicates steady state values):

$$\frac{\bar{\psi}\,\bar{\omega}}{\varepsilon\, v} = \zeta\, \bar{B}_{\omega_{\text{nucleated}}} \tag{50}$$

so that

$$\bar{B}_{\omega_{\text{Total}}} = (\zeta+1)\,\bar{B}_{\omega_{\text{nucleated}}} \tag{51}$$

the sensitivity parameter of the system b/g* for the seeded case will be less than the sensitivity parameter for the unseeded case at identical supersaturations.

$$\frac{b}{g}^{*}_{\substack{\text{seeded}\\ \text{system}}} = \frac{1}{1+\zeta}\,\frac{b}{g} \tag{52}$$

Therefore, at identical supersaturation levels seed addition will increase the stability limits of a crystallizer while at the same time it reduces the Weight Mean Particle Size.

To determine the stability boundaries of the seeded system, when the seed size is different from the nuclei size, one can start with the linearized equations (34). But the associated dimensionless groups Ln, Rn and Sn given in equations (35-37) must be recalculated, taking the seed terms into account (See Appendix 6.2).

In order to evaluate these groups one can simplify matters by making the assumption that the seed distribution is a delta function at seed size r_s such that:

$$\gamma_n = \int_0^\infty \psi(r)\,\delta(r-r_s)\,r^n\,dr = r_s^n\,\psi \tag{53}$$

Then two new steady state dimensionless groups are defined:

$$\beta = \frac{\bar{\omega} r_s}{V \bar{G}} \tag{54}$$

$$\xi = \frac{\bar{\omega}\,\bar{\psi}}{V \bar{\varepsilon} \bar{B}} \tag{55}$$

The first of these, β, is similar to α defined in equation (45) and is the ratio of the seed size to the steady state size increase per draw-down time. The second group ξ is the ratio of the seed addition rate per unit volume of crystallizer to the nuclei generation rate per unit volume of crystallizer. Substituting (45), (54) and (55) into the steady state moment relations (25) simplifies their representation as shown below:

$$\begin{aligned}
\bar{\mu}_0 &= \bar{\varepsilon}\bar{B}\frac{V}{\bar{\omega}}(1+\xi) \\
\bar{\mu}_1 &= \bar{\varepsilon}\bar{B}\frac{V}{\bar{\omega}}\left(\frac{V}{\bar{\omega}}\bar{G}\right)\left[(\alpha+1)+\xi(\beta+1)\right] \\
\bar{\mu}_2 &= \bar{\varepsilon}\bar{B}\frac{V}{\bar{\omega}}\left(\frac{V}{\bar{\omega}}\bar{G}\right)^2\left[(\alpha^2+2\alpha+2)+\xi(\beta^2+2\beta+2)\right] \\
&\text{etc.}
\end{aligned} \tag{56}$$

so that

$$\begin{aligned}
L_n &= n\frac{V}{\bar{\omega}}\bar{G}\frac{\bar{\mu}_{n-1}}{\bar{\mu}_n} = \text{function}(\alpha,\beta,\xi) \\
R_n &= K\frac{\bar{\mu}_3}{\bar{\mu}_n} r_0^n \frac{V}{\bar{\omega}}\bar{B} = \frac{1-\bar{\varepsilon}}{\bar{\mu}_n} r_0^n \frac{V}{\bar{\omega}}\bar{B} = \text{function}(\alpha,\beta,\xi,\bar{\varepsilon}) \\
S_n &= \frac{\gamma_n}{\bar{\mu}_n} = \frac{r_s^n\,\bar{\psi}}{\bar{\mu}_n} = \text{function}(\alpha,\beta,\xi)
\end{aligned} \tag{57}$$

The behaviour of the linearized equations describing the

FIGURE 4

EFFECT OF SEEDING ON STABILITY AND THROUGHPUT

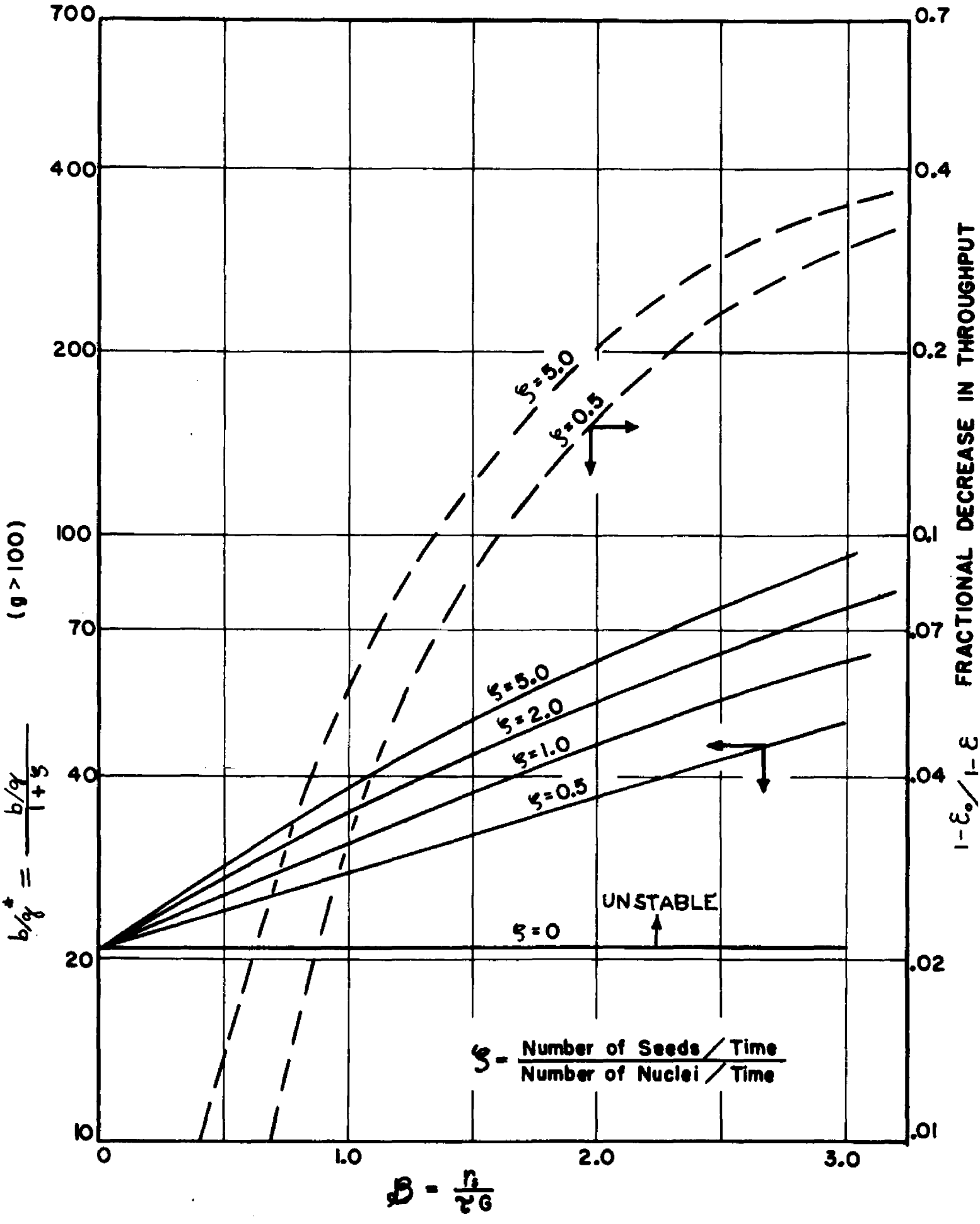

seeded case is determined by the parameters α, β, $\bar{\varepsilon}$, ζ, g and b. The two new groups β, and ζ being added to characterize the seed size and quantity.

The stability boundaries for the seeded feed were investigated for a number of cases and the results are represented in Figure 4. These curves are for a nuclei size of zero (α =o.), and a value of g = 500. The stability boundaries, as in the unseeded case, are relatively insensitive to variations in $\bar{\varepsilon}$ and g (when g is greater than 100). The stability limits increase with increasing seed number and seed size, both of which contribute to increasing surface area. However, large seed sizes ($\beta > 1.0$) are not realistic since for a fixed feed rate or draw-down time the net throughput of product is diminished. Figure 4 also shows this relation by plotting the ratio of the crystal fraction of the feed over that of the product stream, against seed size at two levels of seed addition. The ordinate represent the loss of production capacity due to seeding.

3.43 Effect of Size Dependent Growth Model

In the previous calculations it was assumed that the linear growth rate is independent of size. This assumption is correct if the rate determining step is the kinetic deposition rate at the surface. It has also been shown experimentally that for large crystals ($d >> 100\mu$) the overall mass transfer coefficient at high agitation rates is independent of size. For very small crystals this

assumption probably does not hold. As mentioned previously, if the growth rate is size dependent, the analytical treatment becomes much more complicated as the first four moments equations plus the solute balance equation are no longer a closed set of equations. However it is possible to estimate the nature of the effect of size dependent growth rates on stability by linearizing the growth function G(r, c).
If one can approximate G(r, c) by

$$G(r,c) = \frac{dr}{dt} = G(c)\,\phi(r) = G(c)(1+ar) \qquad (58)$$

then the set of equations (11) and (20) will still give a self-contained set.

When performing the calculations for this case it was assumed that the term $a\bar{v}\bar{G}/\bar{\omega}$ was small, i.e. of the order $\pm$ 0.1 or less. The group $a\bar{v}\bar{G}/\bar{\omega}$ is the relative size increase per draw-down time due to the size dependent term ar , and the assumption that its value remains small is synonymous with the assumption that we are investigating a first order correction of the size independent (ϕ =1.) growth model (See Appendix 6.3).

Figure 5 shows the effect of the size dependent term on the stability contours for non seeded operation with the nuclei size (α) equal to zero. It is seen that a model which predicts increasing growth rate with increasing size raises the system's stability limits. Based on the previous

FIGURE 5

EFFECT OF LINEAR $\phi(r)$ ON STABILITY

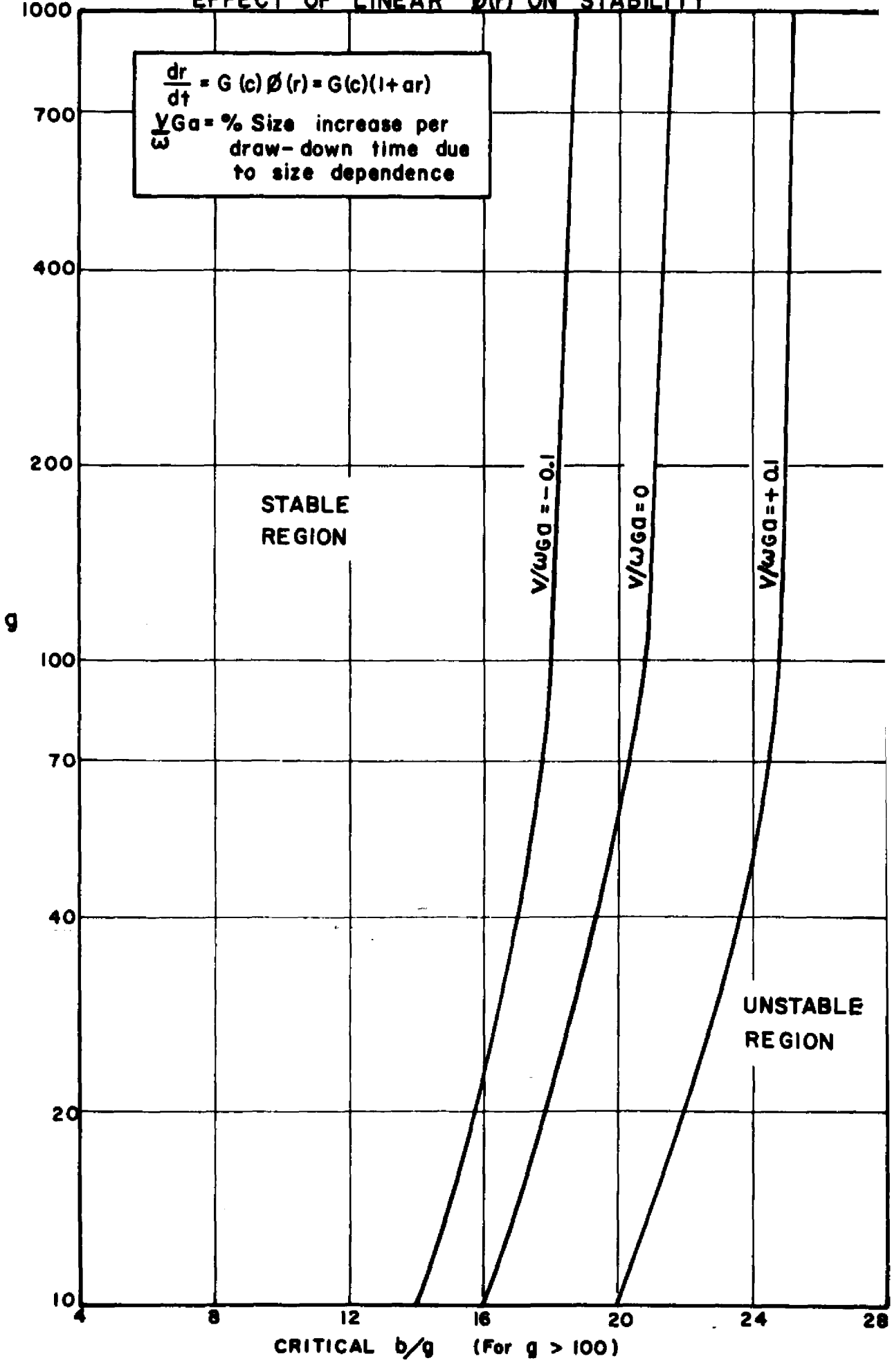

results this is to be expected since it should lead to a shorter time lag between the appearance of increased nuclei and increased surface area in the system.

3.44 Effect of Operation with a Fines Trap

In order to increase crystal product size many crystallization systems utilize a nuclei trap. This usually consists of withdrawing solution from some part of the vessel in such a manner that only crystals below a certain size will be elutriated with the solution. This stream is heated to redissolve the solids and then returned to the crystallizer body. Most often this operation is carried on continuously rather than on the basis of some feedback signal. The question we wanted to answer at present is whether this continuous nuclei removal operation would increase or decrease the system's stability.

In order to dissolve the nuclei it must be trapped very early, before it has a chance to grow, say with 1/8 or $\frac{1}{4}$ of a draw-down time $\tau(\frac{V}{\omega})$. Figure 6 indicates that over this time period, even for cycling behavior, the variation in supersaturation or growth rate G(c) is relatively small. We therefore assume a quasi steady state condition such that the fraction of new nuclei being generated at a specific time which survive the trap can be related to the instantaneous growth rate.

The residence time distribution function F(t) is the fraction of particles which reside in a vessel for a period of time less than t. For a well stirred vessel this function

is

$$F(t) = 1 - e^{-\frac{t}{\tau'}} \tag{59}$$

where τ' is a draw-down time, and for this analysis is based on the volumetric flow to the nuclei trap. If the critical size for removal is denoted as r_c we can denote the fraction of newly formed nuclei lost to the trap as

$$\text{Fraction Lost} = 1 - e^{-\frac{r_c}{G\tau'}} \tag{60}$$

since we have made the quasi steady state assumption over this small time period. Therefore the net nucleation rate for the crystallizer and associated nuclei trap is:

$$\text{Net nucleation} = \mathcal{B}^{(c)} e^{-\frac{r_c}{G\tau'}} \tag{61}$$

To determine the stability of this system we can utilize the previously derived analysis presented in the beginning of this section. All we need do is use equation (61) as the nucleation function in determining the system sensitivity parameter b/g. We see then that for this case

$$b/g^{*} = \frac{\bar{G}\,\frac{d\mathcal{B}^{(\bar{c})}}{dc}}{\bar{\mathcal{B}}\,\frac{dG^{(\bar{c})}}{dc}} + \frac{r_c}{\tau' G} \tag{62}$$

whereas for operation without the fines trap

$$b/g^{*} = b/q = \frac{\bar{G}\,\frac{d\mathcal{B}^{(\bar{c})}}{dc}}{\bar{\mathcal{B}}\,\frac{dG^{(\bar{c})}}{dc}} \tag{63}$$

all the terms being evaluated at the steady state.

At a specified solute concentration the value of equation (62) is always larger than equation (63). Alternately from equation (42) we see that the critical supersaturation level, beneath which cycling occurs, is higher when a nuclei trap is added to the system. Since the steady state solute concentration is slightly increased when a nuclei trap is added to the system, a specification must be set for the two modes of operation before a comparison can be made as to their relative stability.

A meaningful comparison between operation with and without fines trap is to specify that with the same feed composition, the same product should be produced (e.g. the same Weight Mean Particle Size). Since the supersaturation is greater with the operation of a fines trap than without, the production rate will also be greater for this case. It is shown in Appendix 6.4 that for this case, the addition of a fines trap to a crystallizer to produce the same product at a higher capacity will not reduce the stability of the system.

3.5 Non Linear Solutions

3.51 Clear Feed

In the previous section, the stability of the system was analyzed by linearization of the equations. This allows one to predict the general effect of the physical parameters on the system and is especially useful when investigating the possibility of stabilizing such a crystallizer by changing the crystallization conditions, seeding or some feedback control. However, in order to understand the complete behavior of the system it is illuminating to solve the complete non linear set of equations which can only be done numerically (or on an analog computer).

The starting point of the following analysis is the system of equations (22), without the seed terms.

$$\frac{d\mu_n}{dt} = nG\mu_{n-1} + (1-K\mu_3)B r_0^n - \frac{\omega}{V}\mu_n \qquad n=0,1,2,3\ldots \tag{64}$$

$$(1-K\mu_3)\frac{dc}{dt} = \frac{\omega}{V}(c_0-c) - (\rho-c)(3K\mu_2 + (1-K\mu_3)BKr_0^3) \tag{65}$$

To simplify the study of dynamic behaviour of this type of system, the variables are normalized about the steady state variables corresponding to the feed concentration C_0 and rate ω. If the feed concentration and rate vary periodically, their mean values can be used as reference points.

Instead of defining the concentration variable as being the ratio of absolute concentration divided by the steady

state value, which would be extremely close to 1. at all times, the normalized supersaturation will be followed in time.

The following dimensionless groups are defined:

$$Z_n = \frac{\mu_n}{\bar{\mu}_n} \qquad n = 0,1,2,3\ldots \tag{66}$$

$$Y = \frac{C - C_s}{\bar{C} - C_s}$$

where C_s is constant since the system is isothermal.

Since the feed concentration and rate can vary with time, we define:

$$j(\theta) = \frac{\omega(\theta)}{\bar{\omega}}$$

$$h(\theta) = \frac{C_0(\theta)}{\bar{C}_0} \tag{67}$$

$$\theta = t\bar{\omega}/V$$

where $\bar{C}_0$ and $\bar{\omega}$ are the average values of these inputs. If the feed conditions are constant $j(\theta)$ and $h(\theta)$ are 1.

If these groups are substituted in (64) and (65), along with the dimensionless steady state groups defined in (35) and (36), we get:

$$\frac{dZ_n}{d\theta} = L_n\left(\frac{G}{\bar{G}}\right)Z_{n-1} + \left(\frac{B}{\bar{B}}\right)\frac{R_n}{1-\bar{E}} - \left(\frac{B}{\bar{B}}\right)R_n Z_3 - Z_n j(\theta) \tag{68}$$

$$n = 0,1,2,3\ldots$$

and recognizing that $\frac{dC}{dt} = \frac{d(C-C_s)}{dt}$

$$(1-(1-\bar{\varepsilon})Z_3)\frac{d\gamma}{d\theta} = \dot{\gamma}(\theta)\left[h(\theta)\frac{\bar{C}_o - C_s}{\bar{C}-C_s} - \gamma\right] + \gamma(\theta)\left[h(\theta)-1\right]\frac{C_s}{\bar{C}-C_s} - \left[\frac{\rho-C_s}{\bar{C}-C_s} - \gamma\right]\left[L_3\left(\frac{G}{\bar{G}}\right)(1-\bar{\varepsilon})Z_2 + (1-(1-\bar{\varepsilon})Z_3)R_3\left(\frac{\beta}{\bar{\beta}}\right)\right] \quad (69)$$

The two concentration groups in equation (69)

$$\frac{\bar{C}_o - C_s}{\bar{C}-C_s} \qquad \text{and} \qquad \frac{\rho - C_s}{\bar{C}-C_s}$$

can be rearranged in terms of groups previously defined in the stability study. Taking the kinetic growth model to be linear in supersaturation

$$G(c) = K_1(c-c_s) \quad (38)$$

then as before (39)

$$\gamma = \frac{1}{\bar{\varepsilon}}\frac{\bar{C}_o - \bar{C}}{\bar{C}-C_s}$$

and (70)

$$\frac{\bar{C}_o - C_s}{\bar{C}-C_s} = \frac{\bar{C}_o - \bar{C}}{\bar{C}-C_s} + 1 = 1 + \bar{\varepsilon}\gamma$$

and substituting equation (26) (with $\varepsilon_* = 1.0$) into the second group

$$\frac{\rho - C_s}{\bar{C}-C_s} = \frac{\rho-\bar{C}}{\bar{C}-C_s} + 1 = \frac{C_o - \bar{C}}{\bar{C}-C_s}\frac{1}{1-\bar{\varepsilon}} + 1 = \frac{\bar{\varepsilon}}{1-\bar{\varepsilon}}\gamma + 1 \quad (71)$$

also $$\left(\frac{G}{\bar{G}}\right) = \frac{K_1(C-C_s)}{K_1(\bar{C}-C_s)} = \gamma \quad (72)$$

Also, by assuming a Volmer nucleation model, and remembering we are assuming that c/c_s is close to 1, the nucleation rate can be written as:

$$B = K_2 e^{-\frac{K_3}{[\ln c/c_s]^2}} \approx K_2 e^{-\frac{K_3}{(\frac{c}{c_s}-1)^2}} \tag{40}$$

and in conjunction with the linear growth model:

$$\frac{b}{g} = \frac{2K_3}{(\frac{c}{c_s}-1)^2} \tag{42}$$

so we can substitute for the following groups $\frac{c_s}{\bar{c}-c_s}$ and $\frac{B}{\bar{B}}$

$$\frac{c_s}{\bar{c}-c_s} = \left[\frac{b/g}{2K_3}\right]^{1/2} \tag{73}$$

$$\frac{B}{\bar{B}} = e^{\frac{1}{2}\frac{b}{g}(1-\frac{1}{\gamma^2})} \tag{74}$$

and substituting (70-74) back into (68-69)

$$\left.\begin{aligned} \frac{dZ_n}{d\theta} &= \gamma L_n Z_{n-1} + e^{\frac{1}{2}\frac{b}{g}(1-\frac{1}{\gamma^2})}\left[\frac{R_n}{1-\bar{\varepsilon}} - R_n Z_3\right] - Z_n \gamma(\theta) \qquad n=0,1,2,3\ldots \\ (1-(1-\bar{\varepsilon})Z_3)\frac{d\gamma}{d\theta} &= j(\theta)\left[h(\theta)(\varepsilon g+1)-\gamma\right] + j(\theta)\left[h(\theta)-1\right]\left[b/g/2K_3\right]^{1/2} \\ &\quad -\left[\frac{\bar{\varepsilon}}{1-\bar{\varepsilon}}g+1-\gamma\right]\left[L_3\gamma(1-\bar{\varepsilon})Z_2 + (1-(1-\bar{\varepsilon})Z_3)R_3 e^{\frac{1}{2}\frac{b}{g}(1-\frac{1}{\gamma^2})}\right] \end{aligned}\right\} \tag{75}$$

This set of equations describes the behavior of the system relative to its steady state in terms of the parameters used in the linear stability analysis (remembering L_n is a function of α and R_n is a function of α and $\bar{\varepsilon}$). Therefore, with the linear growth model, the modified Volmer nucleation model, and the assumption of steady-state feed conditions ($j(\theta)$ and $h(\theta)$ equal 1.0), we see the relative dynamic behaviour is determined <u>exactly</u> by the same variables which determine stability (α , g , $\bar{\varepsilon}$, b/g), while for time varying feed conditions, the constant K_3 must also be known.

Alternately, if the metastable nucleation model were used, the term ($\frac{B}{\bar{B}}$) could be arranged:

$$\left(\frac{B}{\bar{B}}\right) = \left(\frac{\gamma - 1 + \frac{m}{b/g}}{\frac{m}{b/g}} \right)^m \tag{76}$$

indicating that in comparison to the Volmer model, the behavior of the system depends on an additional parameter m, which does not appear in the linear stability analysis. The advantage of using the Volmer model which, in most cases, fits the data equally well is that the number of dimensionless groups is reduced. We will later show that in this case the behavior of most crystallizers can be characterized by a single dimensionless group b/g.

Equations (68) and (69), along with appropriate nucleation models (72,74)& (76), were solved numerically with the aid of the City College IBM 7040 Computer for various initial perturbations (Appendix 6.5).

In all cases in which the system parameters indicated linear stability, initial perturbations were indeed damped out. Further, it was found that in all cases for which the system parameters indicated linear instability, limit cycles developed for any size perturbation. This indicates that the regions mapped out by the linearized stability analysis are representative of the behavior of the actual system.

Limit cycle behavior is caused by operation at a point where the nucleation function is very sensitive

(high b/g) which causes the system to give rise to a shower of nuclei when the equilibrium concentration has been exceeded. These nuclei then grow supplying so much area for growth that the solute concentration decreases below its equilibrium value. This in turn causes the generation of much less than the equilibrium supply of nuclei. Continued withdrawal of crystals from the system reduces the available area for growth and this causes the solute concentration to rise, which again results in a shower of nuclei and repetition of the cycle. Figure 6 demonstrates just this behavior for a typical limit cycle.

The remainder of the work presented in this section is focussed on studying the properties of these limit cycles.

The majority of the numerical work done with the non-linear system equations (68) and (69) was performed with the modified Volmer nucleation model (74). For this choice of kinetic models (which includes a linear growth model (38)), the non linear system is completely defined by the dimensionless groups used in the linearized stability analysis (α , $\bar{\varepsilon}$, g, b/g).

Other interesting properties were predicted by Figures 1 and 2 which required corroboration by studying the behavior of the non linear system. Specifically, for values of g greater than about one hundred, the linearized

FIGURE 6 TYPICAL LIMIT CYCLE BEHAVIOR

$\alpha = 0 \quad b/g = 50 \quad g = 500 \quad \varepsilon = 0.8$

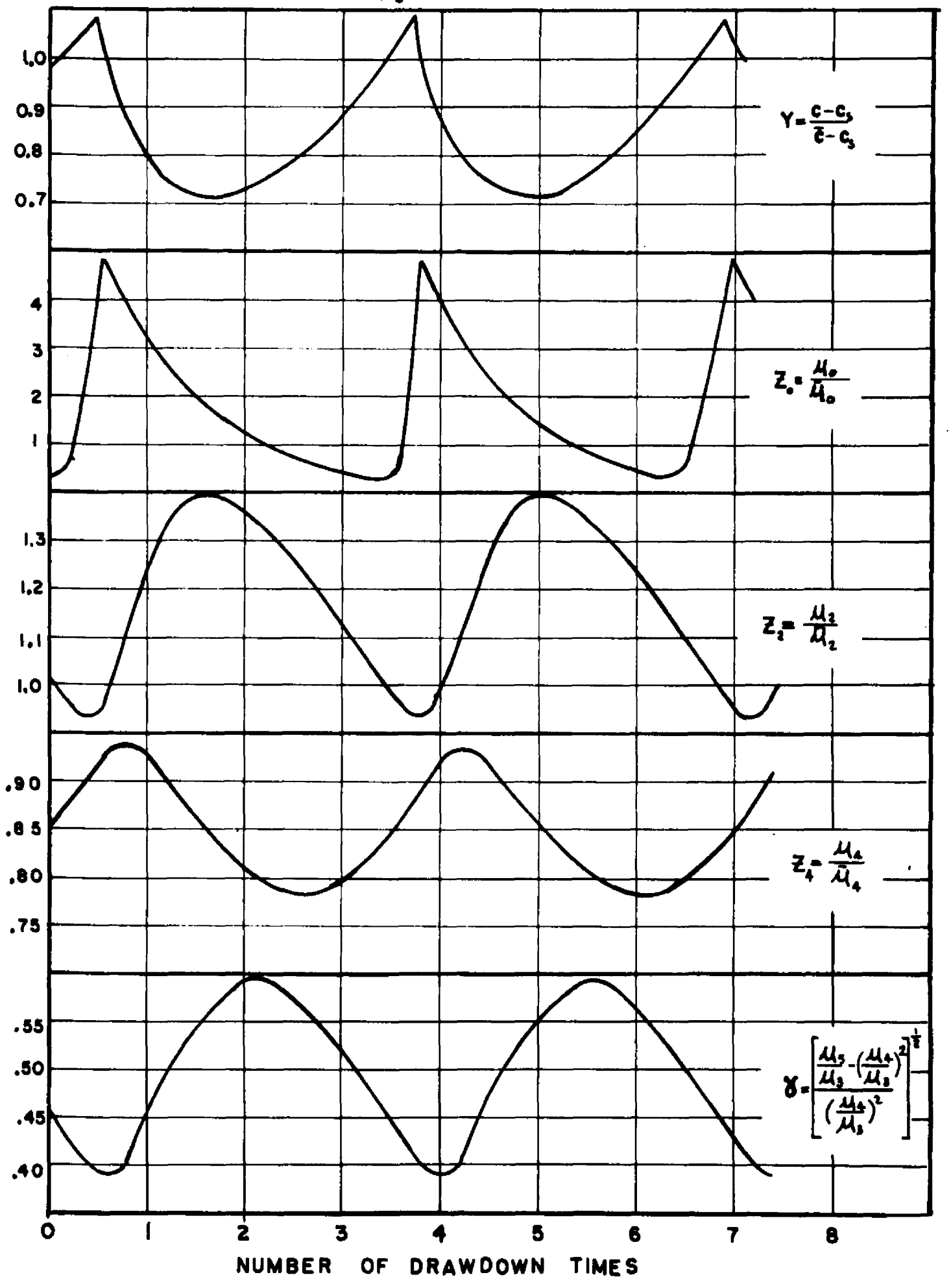

stability study indicated:

a) that the critical value of b/g was independent of g;

b) that the critical value of b/g was independent of $\bar{\epsilon}$

Numerous results did indeed indicate that for moderately high values of g, the normalized dynamic behavior of the system is independent of g and $\bar{\epsilon}$.

Since the assumption of $q_t > 10^2$ is realized for most crystallization systems, the dynamic behavior of the system relative to its predicted steady state becomes a function of only two variables (b/g and α). Then once α has been specified, the value of b/g is the only parameter of importance in determining the system's limit cycle behavior .

It was mentioned previously that for a different choice of the nucleation model such as the metastable model, an additional dimensionless group γ_m was introduced. One would, however, expect from the results based on the modified Volmer model that the effect of changing γ_m , while keeping b/g constant, should be negligible. This is due to the fact that both nucleating functions are similar near the so-called metastable region it would be hard to differentiate between them on the basis of experimental data.

The effect of γ_m on the limit cycle was evaluated by determining numerically how the parameters of the limit cycle

varied as a function of m . For values of g and α for which the critical value of b/g is independent of g and $\bar{\epsilon}$, the effect of changing m on the parameters of the limit cycle was negligible.

Curves describing the behavior of the limit cycles are presented in Figures 7, 8 and 9 for α values of 0.0 and 0.1. Actually, the nuclei formed in most systems are so small that α can be taken to be approximately zero, but the effect of this variable is so great that it was pertinent to show the behavior of systems with values of α up to at least 0.1.

Figure 7 shows the relation between Cycle Time and b/g, and Figure 8 is a graph of the cycle average Relative Weight Mean Size vs. b/g (both for $q_0 > 10^2$). The cycle average Relative Weight Mean Size is the average of $\bar{z}_4/\bar{z}_3$ over a cycle and is indicative of a composite of continuously sampled material.

As the sensitivity of the system increases (b/g gets greater), a small excess value of Y (relative supersaturation) causes a larger amount of new nuclei (the maximum value of the zero moment increases), requiring a longer interval of time to withdraw the crystals before another shower can take place. This increase of b/g also raises the average surface area present over a cycle, thereby lowering the Weight Mean Product Size. Both these effects are show in Figures 7 and 8.

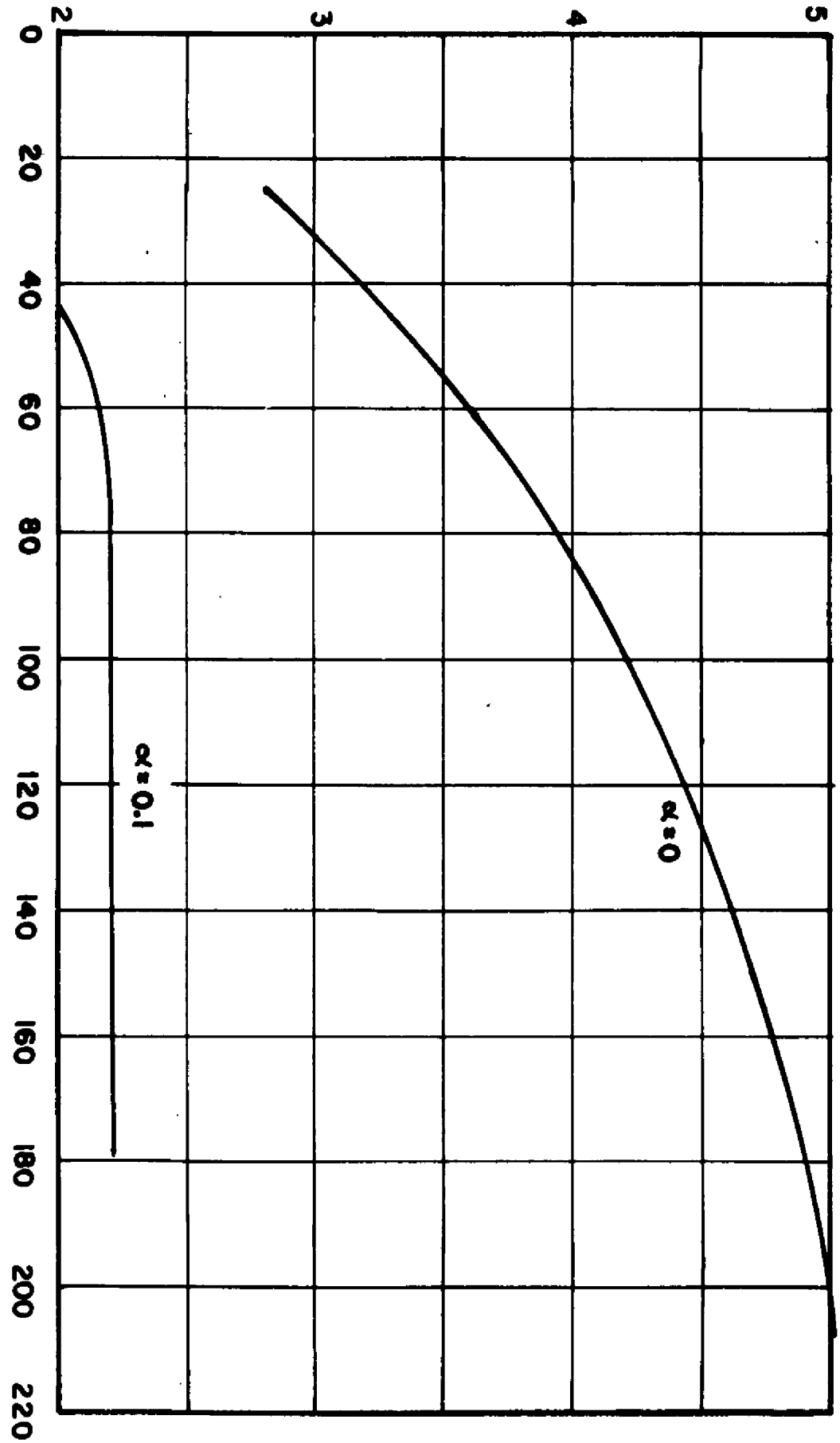

FIGURE 7
CYCLE TIME vs. b/g
FOR g>100

FIGURE 8

CYCLE AVERAGE RELATIVE WEIGHT MEAN SIZE $\frac{z_4}{z_3}$ vs. $\frac{b}{g}$

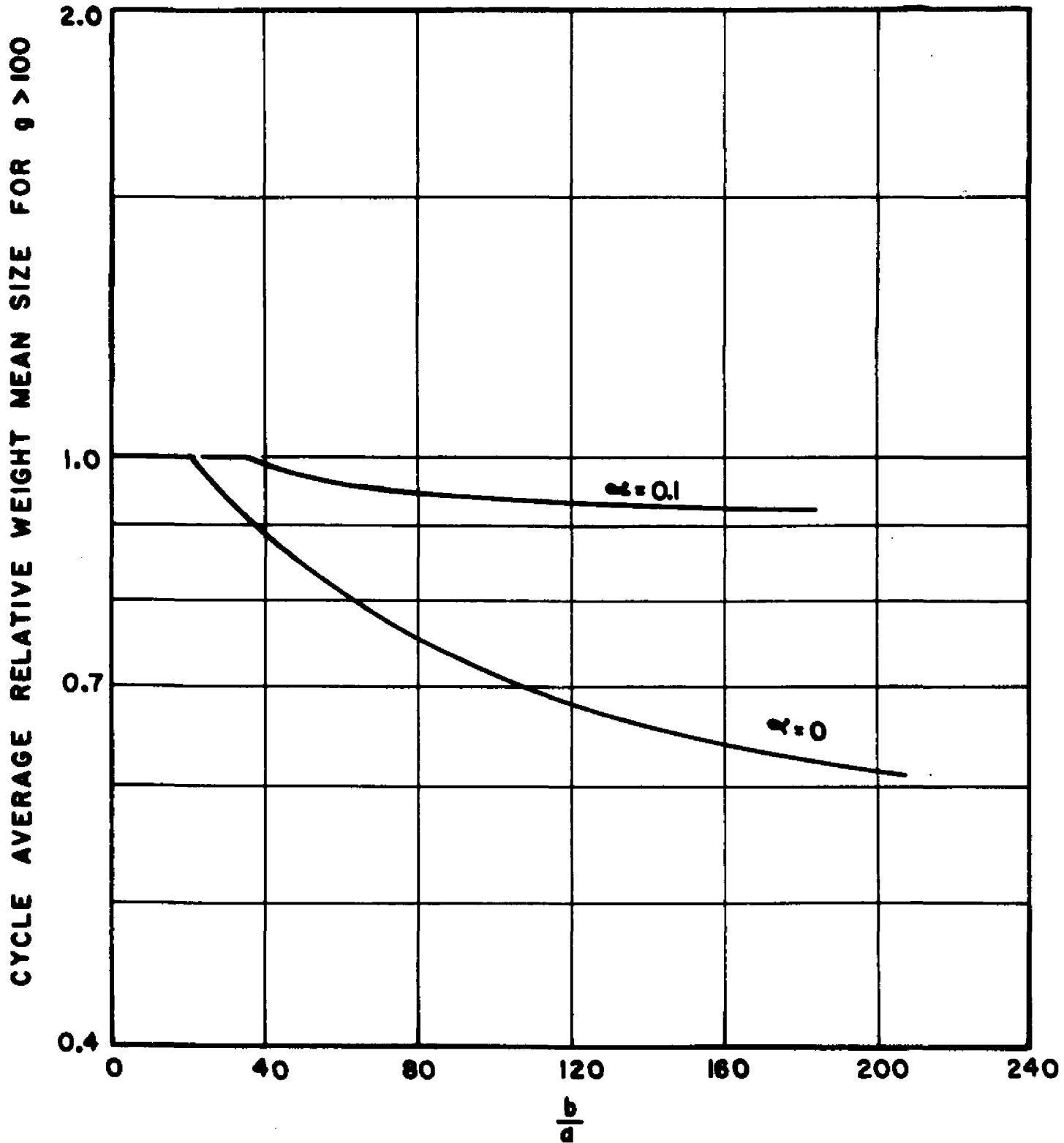

FIGURE 9

CYCLE AVERAGE AND LOCAL COEFFICIENT OF VARIATION OF THE WEIGHT DISTRIBUTION vs. b/g

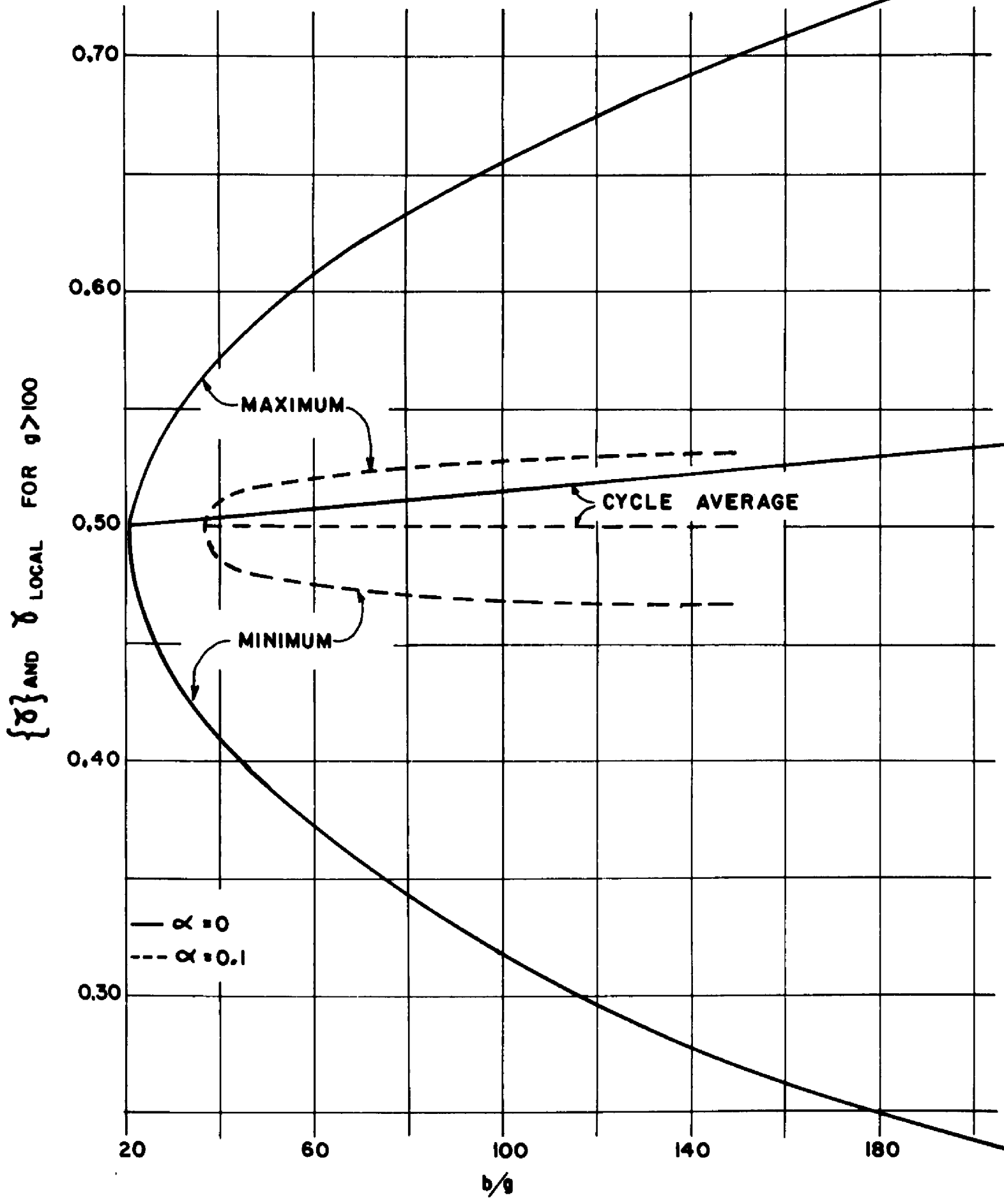

The effect of increasing the size of α is to damp the amplitude of the zero moment. This is due to the increased size of the nuclei which when formed rapidly reduce the supersaturation, causing less nuclei to be formed during a disturbance than would be for a system with an α of zero. This, in turn, means the Cycle Time will be shorter and the Relative Weight Mean Size larger than for a system with a negligible α . This is also shown by Figures 7 and 8.

Figure 9 relates the local and cycle average (composite) Coefficient of Variation of the weight distribution to b/g. This indication of the "tightness" of the distribution is equal to 0.5 for a crystallization system operating in the steady state (both for α = 0.0 and 0.1). It is shown in Appendix 6.6 that the composite value of γ can never be better than the steady state value. The actual composite value of γ , when α = 0.0, is only slightly greater than 0.5, while when α = 0.1 the difference from 0.5 could not even be noticed. Therefore, on a time averaged basis the non stable system givesn nearly as good a product as a stable system.

3.52 Stabilization by Seeding

There is much practical experience in industry which indicates that adding seed to an oscillating crystallizer will stabilize its operation. The results of the last section seem to corroborate this.

If one had an oscillating system at hand it would be interesting to learn just how much seed of what size would be necessary to stop the oscillations and how the resulting product distribution would change. We have performed this analysis for one case where the initial steady state parameters were

$$\alpha = 0.$$
$$\bar{\epsilon} = 0.8$$
$$g = 500$$
$$b/g = 50$$

These parameters represent an unstable system as can be seen from Figure 1. From Figure 8 it is seen that the resulting product distribution has a Cycle Average Weight Mean Size of only 85% of that predicted by the steady state equations. Figure 9 shows that substantial local fluctuations in the coefficient of variation will occur while the resulting average is only slightly higher than that of steady state operation.

To perform the calculation we assumed a linear growth model and modified Volmer nucleation model such that the group b/g is equivalent to that given in equation (42). The volumetric feed rate remained constant and for each seed size a trial and error calculation was performed to determine how much seed was necessary to stabilize the system (See Appendix 6.7). When this was found the Weight Mean Size

relative to that predicted by the initial, but unstable, steady state could be calculated. Other properties such as the coefficient of variation and the feed voidage, the latter being an indication of lost productivity as it becomes less than one, were also calculated.

The results of these calculations are shown in Figure 10. It can be seen that for values of β below 1 there is an imperceptibly small difference in the resulting Weight Mean Size, Variance or Productivity as compared to the initial, but unattainable, steady state values. The reason for this is that the final steady state has a lower supersaturation than the original unseeded steady state had (final b/g equals 54, original equalled 50) which results in a lower nucleation rate, thus tending to offset the effect of seed addition.

It appears therefore that seed addition is an excellent solution to end cycling performance by both stabilizing the operation and increasing the Weight Mean Size of the product without any significant loss of production.

The results of this study can also be used to analyze the performance of an imperfectly mixed crystallizer. For example, poor mixing at the feed inlet would lead to local high supersaturation levels and local high nucleation rates while the rest of the crystallizer is well mixed. This sort of system is analagous to a seeded feed into a well mixed crystallizer, indicating why many commercial installations are free of the problem of cycling.

FIGURE 10

EFFECT OF SEED SIZE STABILIZATION

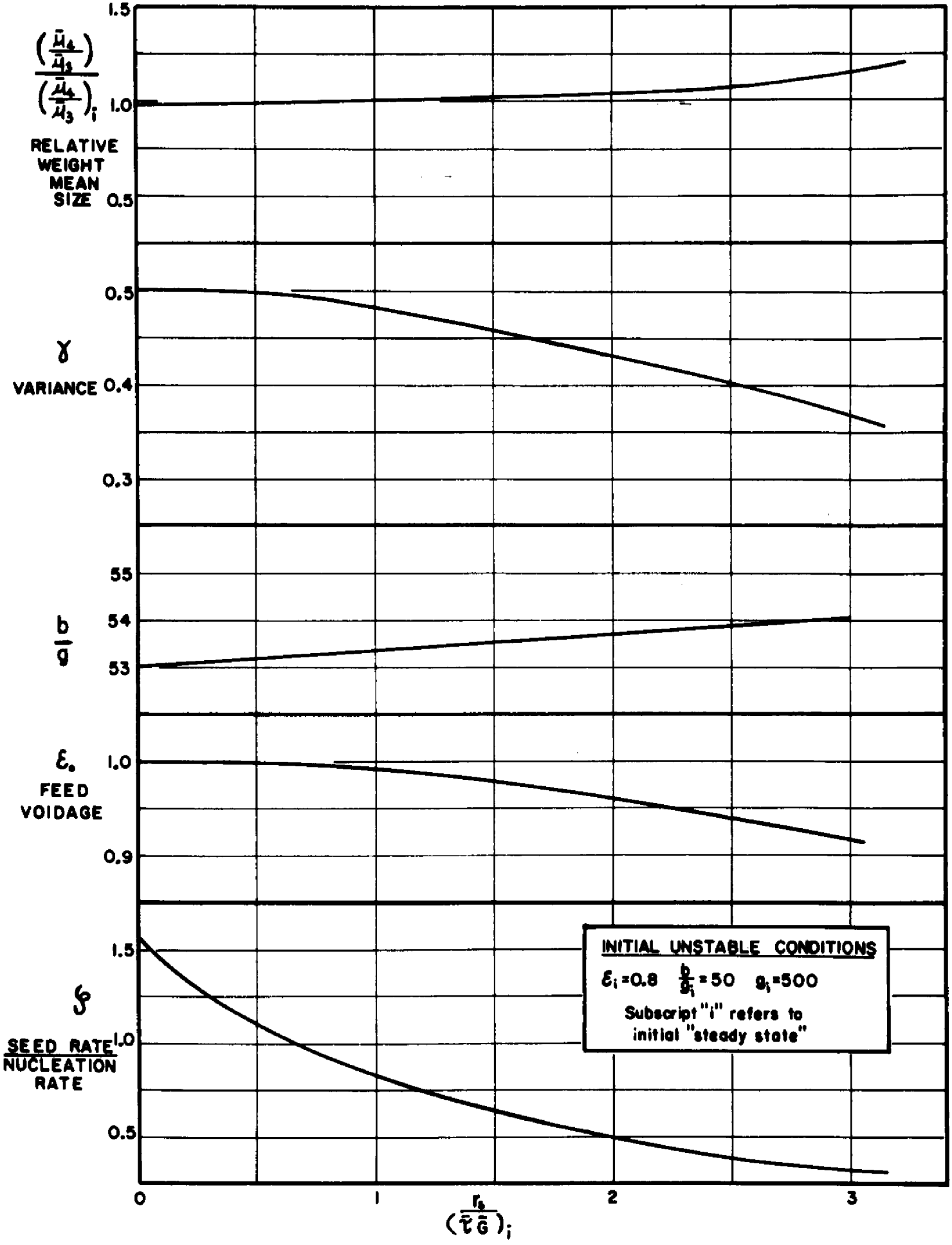

4. Classified Product

4.1 Derivation of the Model

A diagram of the type of operation to be discussed is shown below:

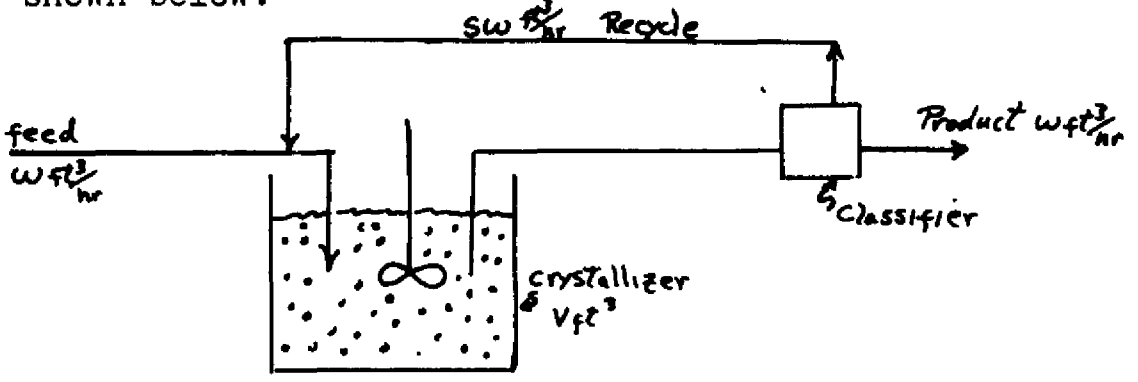

A feed material containing solute at concentration C_o is fed to the crystallizer at a volumetric rate ω . A slurry is withdrawn from the crystallizer body at a volumetric rate $(S + 1)\,\omega$ and sent to a classifying device; the design of which is usually based on centrifugal or elutriative principles. This classifier is designed to produce two separate streams; a product stream of volumetric rate ω which contains all the crystals in the classifier feed which were above a specified critical size r_1 ; and a recycle stream $s\omega$ which contains all the crystals in the classifier feed stream which were below size r_1 .

These classifiers are not so efficient that they perfectly separate all material above and below a specific size r_1 . However, the size range of material which is usually dispersed between the classifier product streams is narrow enough to allow this simplification of our model.

The steady state crystal distribution of the crystallizer body and product stream are qualitatively shown below as a function of the classifier recycle ratio S:

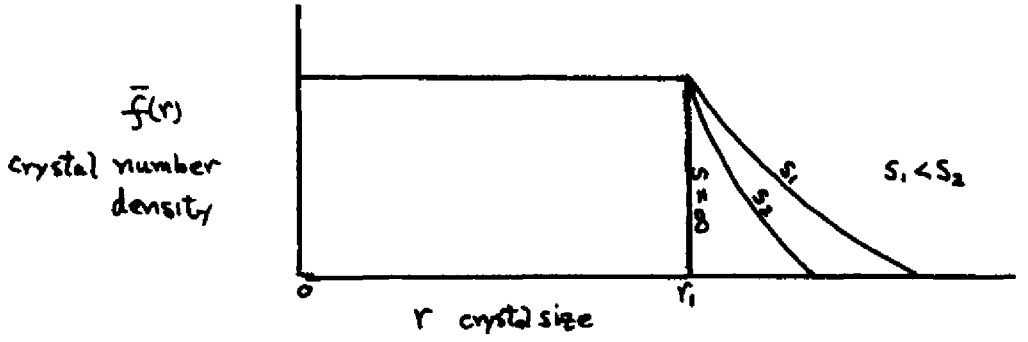

The distribution above size r_1 is exactly the same as the product distribution. As the recycle S increases the tail of material above size r_1 narrows until at an infinite value of S there is no material present in the crystallizer above size r_1 and the product size distribution can be represented by a Dirac delta function at size r_1 .

It has been shown (6) that the product distribution resulting from a value of S equal to 10 is in most cases indistinguishable from the distribution of S equal to infinity. We therefore also make the assumption in our model that S equals infinity since this greatly simplifies the mathematical treatment and normally the classifier recycle ratio will not be far from 10.

The steady state behavior of this model has been described by Saeman (13) and Bransom (2).

In order to describe the behavior of the Isothermal

Mixed Suspension Classified Product Crystallizer, balances must be written for the particles and the crystallizing material.

The same nomenclature and assumptions introduced in section 3.1 are used here. In addition we are also assuming:

(1) that $\phi(r) = 1.0$, so that the kinetic growth term given in equation (3) can be written as:

$$\frac{dr}{dt} = G(c)$$

and is only a function of supersaturation;

(2) that the volumetric feed and product rates are identical, so from equation (8) the crystallizer working volume V is constant;

(3) that the feed is a clear solution;

(4) that the nuclei size is so small it can be taken as equal to zero. (This is not necessary and was not done during the original work. However, now possessing hindsight, we state that, for the classified product case, the nuclei size has little to no effect on the stability or dynamic behavior of the system. In addition, the assumption $r_o = 0$ greatly simplifies the following development.

4.11 Conservation Equations

The appropriate balances can now be written down. (A detailed derivation of the particle balance can be found in reference 7).

Particle Balance

$$\frac{\partial f(r,t)}{\partial t} + G(c)\frac{\partial f(r,t)}{\partial r} = 0 \qquad (77)$$

B.C.

$f(0,t) = \varepsilon B(c)/G(c)$

$f(r,t) = 0 \quad , r > r_1$

These terms represent in order: the accumulation of crystals at size r, and the net flux of crystals at size r due to growth. The boundary condition at size zero equates the generation of particles $\varepsilon B(c)$ to those growing away from size zero, as indicated by the term $f(0,t)G(c)$. The condition for $r > r_1$ corresponds to the assumption of an infinite recycle ratio.

Solute and Crystal Balance

$$\frac{d}{dt}[V\{\varepsilon c + (1-\varepsilon)\rho\}] = \omega c_0 - [(\omega - k r_1^3 V f(r_1,t) G)c - (k r_1^3 V f(r_1,t) G)\rho] \qquad (78)$$

These terms represent in order: the accumulation of solute and crystal, the input of solute by the feed, and the withdrawal of solute and crystal by the classifier product stream. The term ($k r_1^3 V f(r_1,t) G(c)$) represents the volumetric rate of crystal product reaching size r_1 .

We desire a specific differential equation for the concentration C since the kinetic terms for nucleation and growth depend solely on this variable. By multiplying equation (77) by Kr^3 and integrating over r we get the following relation:

$$\frac{d\varepsilon}{dt} = -\sigma G + KGr_1^3 f(r_1,t) \tag{79}$$

where, as before

$$\varepsilon = 1 - \int_0^\infty Kr^3 f\, dr = 1 - K\mu_3 \tag{80}$$

$$\sigma = 3K\int_0^\infty r^2 f\, dr = 3K\mu_2 \tag{81}$$

Substituting equation (79) into (78), we get the following relation for C:

$$\varepsilon\frac{dc}{dt} = \frac{\omega}{V}(c_0 - c) - (\rho - c)\sigma G \tag{82}$$

which we recognize as being identical to equation (9) for the non classified crystallizer.

The working set of equations are now summarized below:

$$\frac{\partial f(r,t)}{\partial t} + G(c)\frac{\partial f(r,t)}{\partial r} = \varepsilon B(c)\delta(r) - Gf(r,t)\delta(r-r_1)$$

$$\varepsilon\frac{dc}{dt} = \frac{\omega}{V}(c_0 - c) - (\rho - c)\sigma G \tag{83}$$

where $\sigma = 3K\int_0^\infty r^2 f\, dr$

4.12 Moment Equations

In section 3, which treated the mixed product case, the generation of moment equations resulted in a closed set of ordinary differential equations which yielded sufficient information about the system and were simpler to solve than the partial differential equation describing the particle balance. In this case, however, the term $f(r_1, t)$, the number density of particles at the cutoff size r_1, prevents the formation of a closed set of equations.

Still, the moment equations provide a simple approach to deriving the system's transfer function and subsequently its stability limits.

The definition of the moments of $f(r, t)$ as given in equation (13) and the physical significance of the moments formerly described are unchanged. It should be noted that, although the upper limit of integration of r is written as ∞ the term $f(r, t)$ is zero above size r_1 .

Multiplying equation (77) by r^n and integrating over the range of r results in the general moments equation:

$$\frac{d\mu_n}{dt} = n\mu_{n-1}G + \varepsilon B\delta(n) - Gf(r_1,t)r_1^n \qquad n=0,1,2,3\ldots \qquad (84)$$

In terms of the moments of $f(r, t)$, equation (82) can be rewritten:

$$\varepsilon\frac{dc}{dt} = \frac{w}{v}(c_0-c) - (\rho-c)3K\mu_2 \qquad (85)$$

where $\varepsilon = 1-K\mu_3$

The leading four moments of (84) plus (85) do not form a closed set because of the term $f(r_i, t)$.

4.13 Steady State Equations

Since we will normalize both the system and linearized equations about their steady states, a diversion to derive the steady state moments is appropriate at this time.

As previously described, the steady state crystal number density is a constant between the nuclei size and the withdrawal size r_i . The crystal number density can be written, (superscript bar refers to steady state values):

$$\bar{f}(r) = \frac{\bar{\mathcal{E}}\bar{B}}{\bar{G}} \qquad 0 \le r \le r_i \tag{86}$$

$$\bar{f}(r) = 0 \qquad r > r_i$$

The steady state moments can be directly calculated from (86).

$$\bar{\mu}_n = \int_0^{r_i} r^n \bar{f}(r)\, dr = \frac{\bar{\mathcal{E}}\bar{B}}{\bar{G}} \frac{r_i^{n+1}}{n+1} \qquad n = 0,1,2,3\ldots \tag{87}$$

Substituting (86) into the steady state form of (84), we get a recursion formula for the moments.

$$\bar{\mu}_n = \frac{n}{n+1} r_i \bar{\mu}_{n-1} \qquad n = 1,2,3\ldots \tag{88}$$

It is relatively simple to derive a relation between the product size and solids' residence time τ_s .

$$\tau_s = \frac{\text{Crystal Holdup Volume}}{\text{Crystal Volumetric Production Rate}} \tag{89}$$

$$\tau_s = \frac{K\bar{\mu}_3}{Kr_1^3 \bar{G}\bar{f}(n)} = \frac{r_1}{4\bar{G}}$$

so that the product is equal to four times the growth per solids' residence time.

$$r_1 = 4\tau_s G \tag{90}$$

which was derived by Saeman (13).

We must distinguish between

(1) feed residence time and solids' residence time;

(2) voidage fraction in the crystallizer and voidage fraction in the product

which usually are not the same for the classified crystallizer.

We denote the voidage fraction of the product by $\bar{\varepsilon}_p$ and from equation (26) it should be given by

$$\bar{\varepsilon}_p = \frac{\rho - c_o}{\rho - \bar{c}} \tag{91}$$

or by

$$(1 - \bar{\varepsilon}_p) = \frac{Kr_1^3 \bar{\varepsilon} \bar{B} V}{\bar{\omega}} \tag{92}$$

where $Kr_1^3 \bar{\varepsilon} \bar{B} V$ is equal to the volumetric rate of production of crystals of size r_1 .

From (89) we can also write the following

$$\tau_S = \frac{(1-\varepsilon)V}{(1-\varepsilon_p)\omega} = \frac{(1-\varepsilon)\tau}{(1-\varepsilon_p)} \tag{93}$$

from which we see that when the crystallizer body voidage and product voidage are equal, the solids and feed residence times are also equal. This is always true for the mixed crystallizer with no classification.

4.2 Linearization of the Model

As before, we will first study the linearized system to ultimately define the regions of stable and unstable behaviour.

The feed concentration can vary in the form:

$$C_o(t) = \bar{C}_o + C_o'(t)$$

The performance variables are represented by

$$\mu_n(t) = \bar{\mu}_n + \mu_n'(t) \qquad n = 0, 1, 2, 3\ldots$$

$$C(t) = \bar{C} + C'(t)$$

$$f(r,t) = \bar{f}(r,t) + f'(r,t)$$

The initial conditions are

$$C(0) = \bar{C}$$

$$\mu_n(0) = \bar{\mu}_n \qquad n = 0, 1, 2, 3\ldots$$

$$f(r,0) = \bar{f}(r) \qquad (94)$$

The kinetic terms for small displacements can be written:

$$B(c) = \bar{B} + \frac{dB}{dC}(\bar{C}).\, C'$$

$$G(c) = \bar{G} + \frac{dG}{dc}(\bar{c}).\, c'$$

The following dimensionless variables are defined:

$$
\left.
\begin{aligned}
Z_n'(\theta) &= \frac{\mu_n'}{\bar{\mu}_n} \qquad n = 0,1,2,3\ldots \\
Y'(\theta) &= \frac{\varepsilon C'}{\bar{C}_0 - \bar{C}} \\
\mathcal{F}'(r,\theta) &= \frac{f'(r,t)}{\bar{f}} \\
\theta &= t/\tau_s \\
g(\theta) &= \frac{C_0'}{\bar{C}_0 - \bar{C}} \\
q &= \frac{\tau}{\tau_s}\frac{\bar{C}_0 - \bar{C}}{\bar{\varepsilon}\,\bar{G}}\frac{dG(\bar{C})}{dC} \\
b &= \frac{\tau}{\tau_s}\frac{\bar{C}_0 - \bar{C}}{\bar{\varepsilon}\,\bar{B}}\frac{dB(\bar{C})}{dC}
\end{aligned}
\right\} \qquad (95)
$$

Substituting relations (91) and (92) into (84) and (85) results in the following linearized equations:

$$
\frac{dZ_n'}{d\theta} - \left[\left(n\frac{\bar{\mu}_{n-1}}{\bar{\mu}_n}\tau_s\bar{G}\right)q + \left(\frac{\bar{\varepsilon}\bar{B}\tau_s}{\bar{\mu}_n}\delta(n)\right)b - \left(\frac{\bar{\varepsilon}\bar{B}\tau_s}{\bar{\mu}_n}r_1^n\right)q\right]Y' \qquad (96)
$$

$$
-\left(n\frac{\bar{\mu}_{n-1}}{\bar{\mu}_n}\tau_s\bar{G}\right)Z_{n-1}' + \left(\kappa B\frac{\bar{\mu}_3}{\bar{\mu}_n}\tau_s\delta(n)\right)Z_3' + \left(\frac{\bar{\varepsilon}\bar{B}\tau_s}{\bar{\mu}_n}r_1^n\right)\mathcal{F}'(r_1,\theta) = 0
$$

$$
n = 0,1,2,3\ldots
$$

$$
\frac{dY'}{d\theta} + \left[\left(\frac{3\bar{\mu}_2\bar{G}}{\bar{\varepsilon}\bar{B}r_1^3}\right)q + \frac{1}{\bar{\varepsilon}}\left(\frac{\rho - \bar{C}_0}{\rho - \bar{C}}\right)\right]Y' + \left(\frac{3\bar{G}\bar{\mu}_2}{\bar{\varepsilon}\bar{B}r_1^3}\right)Z_2' = g(\theta) \qquad (97)
$$

The groups contained within parenthesis in equations (96) and (97) are composed solely of steady state values and can easily be calculated from equations (82) and (86) to (90). Performing this exercise the linearized system equations reduce to the following:

$$\frac{dz_0'}{d\theta} - \left[\frac{(b-q)}{4}\right] y' + \frac{(1-\bar{\varepsilon})}{4\bar{\varepsilon}} z_3' - \frac{\mathcal{F}'(r,\theta)}{4} = 0$$

$$\frac{dz_1'}{d\theta} - \frac{1}{2} z_0' + \frac{1}{2} \mathcal{F}'(r,\theta) = 0 \qquad (98)$$

$$\frac{dz_2'}{d\theta} - \frac{3}{4} z_1' + \frac{3}{4} \mathcal{F}'(r,\theta) = 0$$

$$\frac{dz_3'}{d\theta} - z_2' + \mathcal{F}'(r,\theta) = 0$$

$$\frac{dy'}{d\theta} + \left[\frac{\tau_s/\tau - (1-\bar{\varepsilon})}{\bar{\varepsilon}} + q\right] y' + z_2' = g(\theta)$$

4.3 Stability Analysis

The set of equations (98) cannot yet be analyzed for stability since an additional expression for $\mathcal{F}'(r,\theta)$ is required. To develop this expression we return to the Particle Balance Equation (77). Linearizing and normalizing this expression with the aid of relations (94) and (95) we get:

$$\frac{\partial \mathcal{F}'(r,\theta)}{\tau_s \bar{G}\, \partial \theta} + \frac{\partial \mathcal{F}'(r,\theta)}{\partial r} = 0$$

$$\text{B.C.} \quad \mathcal{F}'(0,\theta) = (b-q)Y' - \left(\frac{1-\bar{\varepsilon}}{\bar{\varepsilon}}\right) Z_3' \tag{99}$$

It is obvious that we cannot get an ordinary differential expression for $\mathcal{F}(r,\theta)$ from (99). Therefore, we turn to the transfer function to examine the system's stability boundaries. The partial differential equation indicates that the transfer function will contain an exponential function.

Taking the LaPlace transform of equation (99) with respect to θ and denoting the transform by the superscript $\wedge$:

$$\frac{s\,\hat{\mathcal{F}}'(r,s)}{\tau_s \bar{G}} + \frac{\partial \hat{\mathcal{F}}'(r,s)}{\partial r} = 0$$

$$\text{BC.} \quad \hat{\mathcal{F}}'(0,s) = (b-q)\,\hat{Y}'(s) - \left(\frac{1-\bar{\varepsilon}}{\bar{\varepsilon}}\right)\hat{Z}_3'(s) \tag{100}$$

Solving (100), we get:

$$\hat{\mathcal{F}}'(r,s) = \left[(b-q)\,\hat{Y}'(s) - \left(\frac{1-\bar{\varepsilon}}{\bar{\varepsilon}}\right)\hat{Z}_3'(s)\right] C^{\frac{-s\,r}{\tau_s \bar{G}}} \tag{101}$$

and using equation (90) we finally get an expression for $\hat{\mathcal{F}}'(r_1,s)$:

$$\hat{\mathcal{F}}'(r_1,s) = \left[(b-g)\hat{y}'(s) - \left(\frac{1-\bar{\epsilon}}{\bar{\epsilon}}\right)\hat{z}_3'(s) \right] e^{-4s} \qquad (102)$$

Combining (102) with the LaPlace transforms of (98), we get the following characteristic matrix:

Characteristic Matrix

Variable →	$\hat{z}_0'$	$\hat{z}_1'$	$\hat{z}_2'$	$\hat{z}_3'$	$\hat{y}'$	$\hat{\mathcal{F}}'(r_1,s)$	Disturbance
Equation ↓							
0 moment	s	0	0	$\frac{1-\bar{\epsilon}}{\bar{\epsilon}}(\frac{1}{4})$	$-(b-g)/4$	$\frac{1}{4}$	0
1 moment	$-\frac{1}{2}$	s	0	0	0	$\frac{1}{2}$	0
2 moment	0	$-\frac{3}{4}$	s	0	0	$\frac{3}{4}$	0
3 moment	0	0	-1	s	0	1	0
Solute Bal.	0	0	1	0	$s+q+\frac{[\tau_3/\tau - (1-\bar{\epsilon})]}{\bar{\epsilon}}$	0	$\hat{g}(s)$
$\hat{\mathcal{F}}'(r_1,s)$	0	0	0	$\frac{1-\bar{\epsilon}}{\bar{\epsilon}}$	$-(b-g)$	e^{4s}	0

(103)

When multiplying out this matrix, we find the denominator of any transfer function will have the following characteristic equation:

$$A_5 s^5 + A_4 s^4 + A_3 s^3 + A_2 s^2 + A_1 s + A_0 + e^{-4s}(B_4 s^4 + B_3 s^3 + B_2 s^2 + B_1 s + B_0) \qquad (104)$$

The coefficients of this term are functions of the steady state parameters b, g, $\bar{\epsilon}$, and τ_3/τ . (If the nuclei

size were left as a variable, an additional parameter of the form $\tau_0/\tau_s\xi$ would also be present.)

The stability limits of this transfer function were investigated by use of Nyquist diagrams, actual solution for the roots, and the determination of crossover points of the roots over the imaginary axis. These techniques are described in detail in reference (4) and are further discussed in Appendix 6.8.

As in the unclassified case, it was found that the term b/g was the crucial parameter which determined the stability of the system. It was found that the stability contour of b/g was insensitive to changes in g and τ_s/τ , but did vary slightly with changes in $\bar{\xi}$. These limits are shown in Figure 11. It is seen that the critical values of b/g are about 1 to 3 for classified operation, whereas for the unclassified operation, it was about 20. The addition of a classifying device therefore drastically reduces the system's stability.

4.31 Effect of Operating Variables on Stability

The independent variables that an operator has at his control for our model classified crystallizer are temperature, feed rate, product size and fraction of nuclei destroyed (if a fines trap is included). The present paper treats an isothermal case so that the temperature effect has been disregarded. (It should be pointed out that, al-

FIGURE II

STABILITY LIMITS FOR THE WELL MIXED CLASSIFIED PRODUCT CRYSTALLIZER

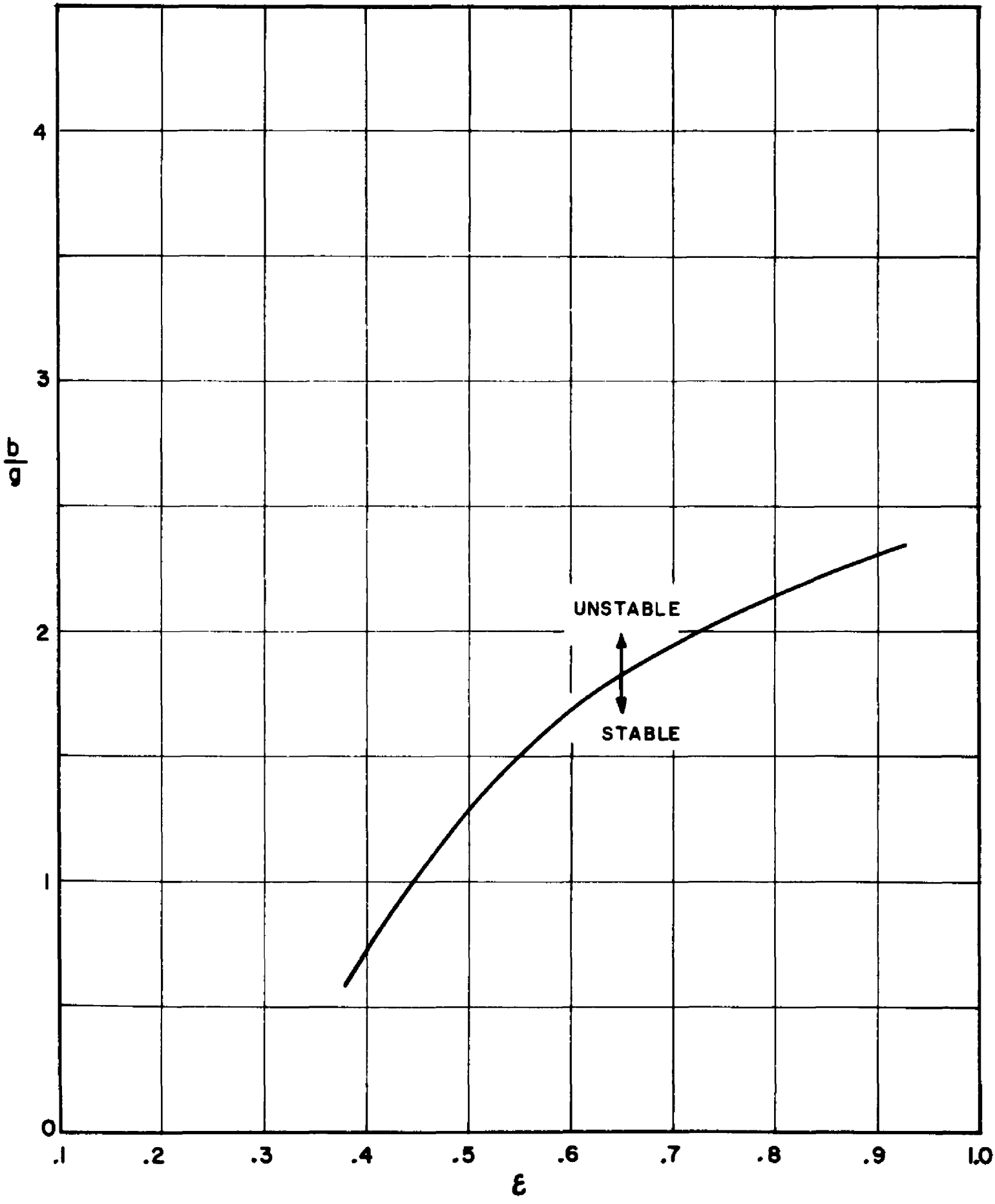

though some papers deal with the effect of temperature on growth rate, there are none that do the same for nucleation of solute from solution.)

Assuming that the fines trap operation is held constant, such that the same fraction of nuclei survive the trap, we would like to investigate:

(1) the effect of varying production rate with constant product size;

(2) the effect of varying product size with constant production rate on the system's stability.

(1) Varying Production Rate

Since the supersaturation is so small when compared to the concentration change between feed and product, we can assume that the volume fraction of solids in the product stream will remain unchanged. From equation (92) we see that, assuming constant product size r_1, this means:

$$\frac{\bar{\varepsilon}_1 \bar{B}_1}{\bar{\omega}_1} = \frac{\bar{\varepsilon}_2 \bar{B}_2}{\bar{\omega}_2} \tag{105}$$

Also, constant product size denotes (from equation (90) and (93)):

$$\tau_{s_1} \bar{G}_1 = \tau_{s_2} \bar{G}_2$$

$$(1-\bar{\varepsilon}_1)\frac{\bar{G}_1}{\bar{\omega}_1} = \frac{(1-\bar{\varepsilon}_2)\bar{G}_2}{\bar{\omega}_2} \tag{106}$$

Solving for $\bar{\omega}_1/\bar{\omega}_2$ from (106) and substituting into (105) gives:

$$\frac{\bar{\varepsilon}_1 \bar{B}_1}{(1-\bar{\varepsilon}_1)\bar{G}_1} = \frac{\bar{\varepsilon}_2 \bar{B}_2}{(1-\bar{\varepsilon}_2)\bar{G}_2} = \text{constant} \tag{107}$$

Assuming a linear growth model as given in equation (38) and a Volmer type nucleation model as given in equation (40), we can use the definition given for b/g in equation (42). In terms of b/g the ratio for growth and nucleation rates take the following forms:

$$\frac{\bar{G}_1}{\bar{G}_2} = \left[\frac{(b/g)_2}{(b/g)_1}\right]^{\frac{1}{2}} \tag{108}$$

$$\frac{\bar{B}_1}{\bar{B}_2} = e^{\frac{1}{2}\left[(b/g)_2 - (b/g)_1\right]} \tag{109}$$

Substituting (108) and (109) into (107)

$$\frac{\bar{\varepsilon}_1}{1-\bar{\varepsilon}_1}(b/g)_1^{\frac{1}{2}} e^{-\frac{1}{2}(b/g)_1} = \frac{\bar{\varepsilon}_2}{1-\bar{\varepsilon}_2}(b/g)_2^{\frac{1}{2}} e^{-\frac{1}{2}(b/g)_2} = \text{constant} \tag{110}$$

Starting with a stable base point, say $\varepsilon_1 = 0.70$, $(b/g)_1 = 1.50$, we can solve (110) for other combinations of ε_2 and $(b/g)_2$ and then from either (105) or (106) determine the relative production rate $\frac{\bar{\omega}_2}{\bar{\omega}_1}$.

Figure 12 plots this curve of b/g versus ε for varying production rates through the base point $\varepsilon_1 = 0.70$, $(b/g)_1 = 1.50$. The stability boundary is shown on the same graph. It can be seen that if the original system is stable,

decreasing the production rate while maintaining a constant product size (and constant fines trap operation) will lead towards an unstable situation.

(2) Varying Product Size

By the same reasoning as before we expect the solids content of the product stream to be essentially constant. And from equation (92) with constant production rate, we see

$$(r_1)^3 \bar{\varepsilon}_1 \bar{B}_1 = (r_1)_2^3 \bar{\varepsilon}_2 \bar{B}_2 = \text{const.} \qquad (111)$$

From equation (90) it can also be shown that

$$(r_1)_1 / (1-\bar{\varepsilon}_1)\bar{G}_1 = (r_1)_2 / (1-\bar{\varepsilon}_2)\bar{G}_2 = \text{const.} \qquad (112)$$

And using equations (108-109) we can follow the same method to determine the variation of ε and b/g and relative size, when starting with the same base point. This is also shown in Figure 12.

It can be seen that increasing the product size while maintaining a constant production rate (and constant fines trap operation) will lead to an unstable situation.

If it is desired to maintain a constant growth rate (constant b/g) when varying production rate or product size, similar analysis to the above show:

(1) A smaller fraction of nuclei should be dissolved in the fines trap when increasing production. (constant product size);

(2) A larger fraction of nuclei should be

FIGURE 12

VARIATION OF b/g AND ε WITH CHANGING PRODUCT SIZE OR PRODUCTION RATE

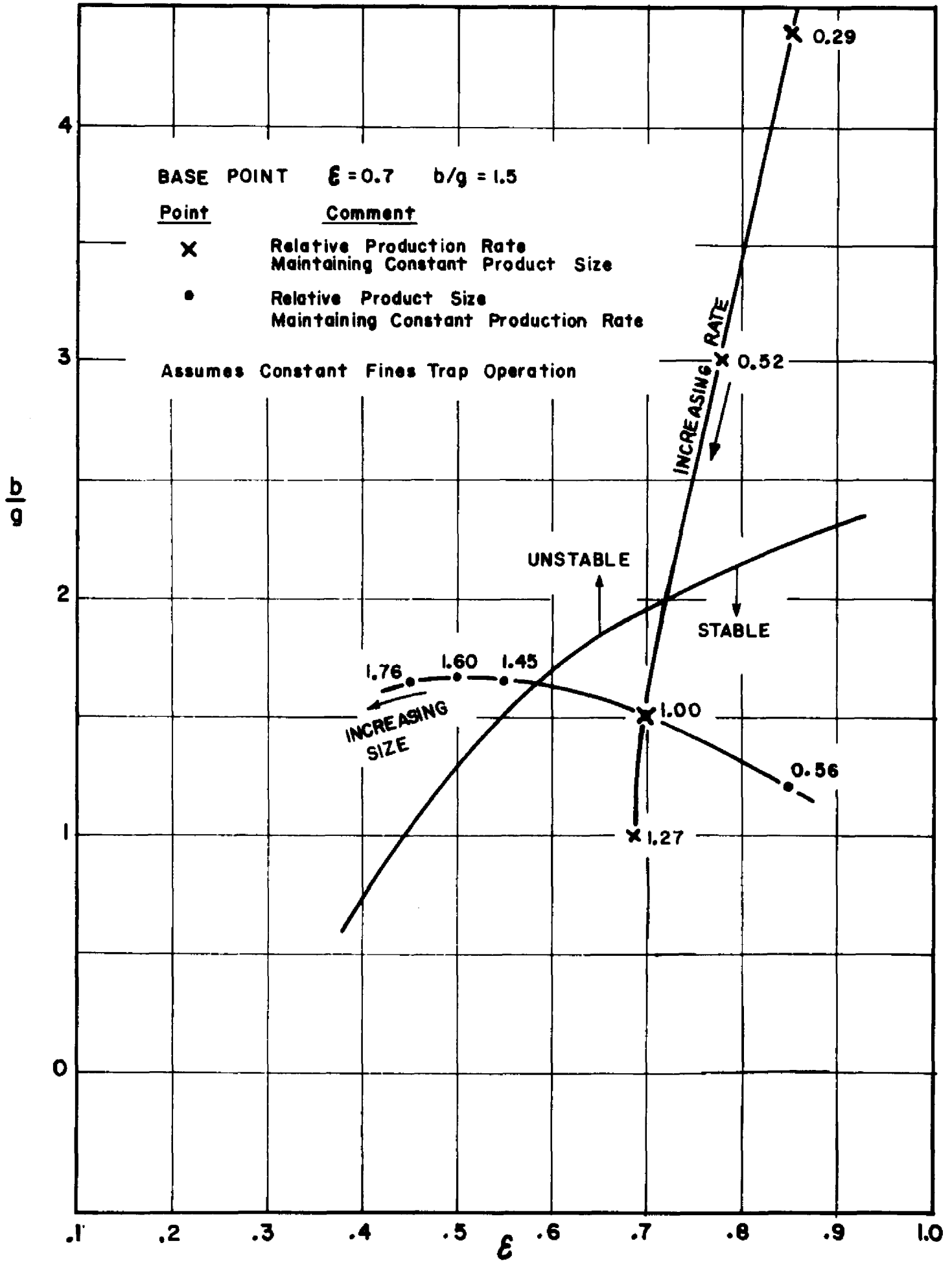

dissolved in the fines trap when increasing product size. (constant production rate)

4.32 Comparison of Mixed versus Classified Operation

The only valid way to compare these two modes of operation is on the basis that they:

(1) operate on the same feed concentration and rate (equal production);

(2) produce the same weight mean product size.

In this section subscript M will indicate mixed operation and subscript c classified operation.

The weight mean particle size for mixed operation is equal to $\bar{\mu}_4/\bar{\mu}_3$ (see equation(16)), while for classified operation it must be equal to the cutoff size r_1 . From equation (25) we can evaluate $\bar{\mu}_4/\bar{\mu}_3$ (with a clear feed and $r_0 = 0$):

$$\frac{\bar{\mu}_4}{\bar{\mu}_3} = 4\tau \bar{G}_M = r_1 = 4\tau_s \bar{G}_c \tag{113}$$

The last part of (113) is obtained by substitution of equation (90).

The number of surviving nuclei required is equal to the production rate divided by average size per product crystal.

$$(\text{Net})Bc = \frac{\text{Production Volume}}{K r_1^3} \tag{114}$$

$$(\text{Net})Bm = \frac{\text{Production Volume}}{K \bar{\mu}_3/\bar{\mu}_0} \tag{115}$$

By net Bc we mean the number of nuclei generated multiplied by the percent surviving the fines trap. A fines trap may or may not be used with mixed product removal, but, as we shall see, under most conditions it is required for classified product removal.

Dividing (114) by (115) and substituting for from (25) we get:

$$\frac{(\text{Net})Bc}{(\text{Net})Bm} = \frac{K\bar{M}_3/M_0}{K r_1^3} = \frac{6(\tau \bar{G}_M)^3}{r_1^3} \tag{116}$$

Substituting (113) into (116):

$$\frac{(\text{Net})Bc}{(\text{Net})Bm} = \frac{6}{64} = 0.094 \tag{117}$$

which was derived by Saeman (13) under somewhat more limiting conditions.

To achieve this reduced nucleation rate requires the addition of,or the improved operation of,a fines trap for the classified case.

Rearranging equation (113) with the aid of equation (93) and (108):

$$\frac{1-\bar{\epsilon}_M}{1-\bar{\epsilon}_c} = \frac{\bar{G}_c}{\bar{G}_M} = \left[\frac{(b/q)_M}{(b/q)_c}\right]^{\frac{1}{2}} \tag{118}$$

Therefore, assuming that ϵ_M is known and no fines trap is used for mixed operation, for every ϵ_c we choose we can

calculate the relative (b/g)c as compared to the sensitivity coefficient for mixed operation. Assuming $\bar{\varepsilon}_m = 0.8$ we get

$\bar{\varepsilon}_c$	(b/g)c/(b/g)m	Required Nuclei Removal
0.7	2.25	<90.6%
0.8	1.0	90.6%
0.9	0.25	>90.6%

Let us focus on the problem of stability. From the results of section 4.3 we see that the region of stable operation for the classified case is much smaller than for the mixed product case. It is therefore quite reasonable to expect that a system which is stable for mixed product operation (b/g < 21) may not be stable for classified operation ($b/g > 2.5$).

Even if (b/g)m is lower than 2.0, switching to classified operation such that conditions (1) and (2) of this section are met will require that (NetBc)/Bm = 0.094 or that a fines trap will be required. Utilizing the relations derived in section 3.44 we see that for fines trap operation:

$$\left(\frac{b}{g}\right)^* = \frac{\bar{G}}{\bar{B}} \frac{\frac{dB}{dC}(\bar{c})}{\frac{dG}{dC}(\bar{c})} + \frac{r_c}{\tau' \bar{G}} \qquad (62)$$

and for the case where the growth rates for mixed and classified operation are held constant (as discussed by Saeman (13)) the term $r_c/\tau'\bar{G}$ will equal 2.36. Therefore, the contribution of this term is itself sufficient to lead to in-

stability.

Therefore, although an ideally mixed system may be stable during non classified operation, it most likely will become unstable if it is converted to classified operation.

If the mixing is not ideal, but has localized high supersaturations at the feed inlet, then this has the same effect as seeding and has a strong stabilizing influence as will be shown in the following section.

4.33 The Effect of Seed Addition

Using the same nomenclature introduced in equation (55) we let ζ represent the ratio of the seed nuclei fed per volume of solution to generated nuclei per volume of solution (at the calculated steady state).

$$\bar{B}_{TOTAL} = \bar{B}^{0}_{NUCLEATED} + B_{SEED} = (1+\zeta)\bar{B}^{0}_{NUCLEATED} \qquad (119)$$

We saw in sections 3.42 and 3.52 that for the mixed case, seeding increased the stability of the system with little deleterious effect on product size. This was because the seeding increased the crystal surface area which lowered the supersaturation and hence the nucleation rate. The total nuclei then were only slightly more than the sum of the seed nuclei and the originally generated nuclei.

In the classified crystallizer we have control over the crystal surface area (or magma density) and can make this trade of generated nuclei for seeded nuclei more easily.

To illustrate, let us assume we are operating a classified crystallizer to produce the same weight mean size crystal as was realized in a non classified operation. Then as was shown in the last section, a fines trap must be added to the system. Then we saw:

$$\left(\frac{b}{g}\right)^* = \frac{\bar{G}}{\bar{B}} \frac{\frac{dB_{(\bar{L})}}{dC}}{\frac{d\bar{G}_{(\bar{L})}}{dC}} + \frac{r_c}{\tau' \bar{G}} \tag{62}$$

$$\left(\frac{b}{g}\right)^* = \frac{b}{g} + \frac{r_c}{\tau' \bar{G}}$$

Now if the system is seeded, the system sensitivity parameter becomes:

$$\left(\frac{b}{g}\right)^* = \frac{\frac{b}{g} + \frac{r_c}{\tau' \bar{G}}}{1 + \mathcal{E}} \tag{120}$$

Say the classified system was unstable (i.e. $\mathcal{E} = 0.9$, $b/g = 5$, $r_c/\tau' \bar{G} = 2.36$ and $(b/g)^* = 7.36$). There is not much we could do to stabilize the operation while still producing the same volume and size product, (other than install a feedback control system). With seeding, we could raise the solids fraction so that only a minor portion of the nuclei are dependent on the supersaturation.

To produce the same size and number of crystals as was originally intended, the nuclei introduced must be the same:

$$\mathcal{E}\mathcal{B} = \text{constant} \quad (\omega \text{ is the same}) \tag{105}$$

and from (106):

$$\tau_s \bar{G} = \text{constant}$$

$$(1-\bar{\varepsilon})\bar{G} = \text{constant} \tag{106}$$

By lowering $\mathcal{E}$ to 0.8 we can use equations (106), (108) and (109) to calculate that now (b/g) = 20 and the generated nuclei are almost nill ($\simeq 5(10^{-3})$ times the original number). The nuclei are now almost exclusively supplied by seed (calculated from (105)) and the fines trap need only be operated if the amount of seed is excessive.

if ζ = 198 $\quad \frac{r_c}{\tau \bar{G}} = 0$ and (b/g) = 0.1

if ζ = 500 $\quad \frac{r_c}{\tau \bar{G}} = 0.91$ and (b/g) = 0.04

It is evident therefore that one might stabilize the classified crystallizer by seeding and yet not suffer a loss in product size.

4.4 Non Linear Solutions

We wanted solutions to the non linearized system equations in time to firstly check the model's behavior in the regions outlined by the stability analysis and secondly to study the characteristics of the limit cycles in the unstable region.

The starting point of this work was the set of equations (82) reproduced below:

Particle Balance

$$\frac{\partial f(r,t)}{\partial t} + G(c)\frac{\partial f(r,t)}{\partial r} = 0$$

B.C.

$$f(0,t) = \frac{\varepsilon B_0}{G(c)} \quad , \quad f(r>r_1,t) = 0 \tag{121}$$

Concentration Balance

$$\varepsilon \frac{dc}{dt} = \frac{\omega}{V}(c_0 - c) - (\rho - c)3KG(c)\mu_2 \tag{122}$$

We did not bother to work with the moment equations for this study since we saw before that for this case they do not lead to a closed set of ordinary differential equations. Therefore, the solution of a partial differential equation will be required to follow the dynamics of this system.

To simplify the study of the dynamic behavior of the system, the variables are normalized about the steady state

variables corresponding to the feed concentration C_0 and rate ω .

The following dimensionless groups are defined:

$$\mathcal{F}(l,\theta) = \frac{f(l,\theta)}{\bar{f}} = \frac{f(l,\theta)}{\bar{\epsilon}\bar{B}/\bar{G}}$$

$$Y = \frac{C-C_s}{\bar{C}-C_s}$$

$$l = r/r_1 \qquad (123)$$

$$\theta = t/\tau_s$$

$$Z_n = \frac{\mu_n}{\bar{\mu}_n} \qquad n = 0,1,2,3\ldots$$

Substituting (123) into (122) along with (87-90) results in the following dimensionless equations:

Normalized Particle Balance

$$\frac{\partial \mathcal{F}(l,\theta)}{\partial \theta} + \frac{1}{4}\frac{G}{\bar{G}}\frac{\partial \mathcal{F}(l,\theta)}{\partial l} = 0$$

B.C.

$$\mathcal{F}(0,\theta) = \frac{(B/\bar{B})}{(G/\bar{G})}\left[\frac{1-(1-\bar{\epsilon})Z_3}{\bar{\epsilon}}\right] \qquad (124)$$

$$\mathcal{F}(l>1,\theta) = 0$$

Normalized Concentration Balance

$$\left(1-(1-\bar{\epsilon})Z_3\right)\frac{dY}{d\theta} = \frac{\tau_s}{\tau}\left[\frac{C_0-C_s}{\bar{C}-C_s} - Y\right] - \left[\frac{C-C_s}{\bar{C}-C_s} + 1 - Y\right]\left[\frac{G}{\bar{G}}(1-\bar{\epsilon})Z_2\right] \qquad (125)$$

where

$$Z_n = (n+1)\int_0^1 l^n \mathcal{F}(l,\theta)\,dl \qquad n=0,1,2,3\ldots \qquad (126)$$

As in the non classified case, we now assume a linear growth model (equation (38)) and a Volmer type nucleation model (equation (40)), so we can use expressions (38) and (42) for g and b/g respectively. Following the same analysis as in the previous section we can incorporate equations (70-72) into (125) and use equation (74) for the term B/$\bar{B}$.

With the incorporation of these kinetic models our working set of equations assumes the following form:

Normalized Particle Balance

$$\frac{\partial \mathcal{F}(l,\theta)}{\partial \theta} + \frac{1}{4} Y \frac{\partial \mathcal{F}(l,\theta)}{\partial l} = 0$$

B.C.

$$\mathcal{F}(0,\theta) = \frac{(B/\bar{B})}{Y}\left[1-\frac{(1-\bar{\varepsilon})z_3}{\bar{\varepsilon}}\right], \quad \mathcal{F}(l>1,\theta) = 0$$

Normalized Concentration Balance (127)

$$\left[1-(1-\bar{\varepsilon})z_3\right]\frac{dY}{d\theta} = \varepsilon q + \frac{\tau_s}{\tau}(1-Y) - \left[\frac{\bar{\varepsilon}}{1-\bar{\varepsilon}} q + 1 - Y\right]\left[Y(1-\bar{\varepsilon})z_2\right]$$

where

$$z_n = (n+1)\int_0^1 l^n \mathcal{F}(l,\theta)\, dl \qquad n = 0,1,2,3\ldots$$

$$\frac{B}{\bar{B}} = e^{\frac{1}{2}\frac{b}{g}\left[1-\frac{1}{Y^2}\right]}$$

The steady state parameters which determine the normalized dynamic behaviour of the system are $\bar{\varepsilon}$, τ_s/τ, g, b/g; the same groups which determined the stability regions in the linearized analysis.

As in the linearized study, it was found that changing the values of τ_s/τ and g had a very

small effect on the normalized dynamic behavior and the parameters $\bar{\varepsilon}$ and b/g were of primary significance.

The technique used for the solution of (127) is discussed in Appendix 6.9.

Numerical solutions corroborated the linearized analysis in that for all systems where parameters indicated stable operation, initial perturbations damped out, regardless of the size of the perturbation. As expected for all systems whose parameters indicated linear instability, initial perturbations from steady state grew into well defined limit cycles.

The characteristics of a typical limit cycle are shown in Figure 13. Figure 14 illustrates the fluctuations in the normalized particle densities over the limit cycle.

From Figure 13 we see that the same internal feedback mechanism is prevalent in the classified operation as for the non classified case, except that in this case the crystal density distribution varies in the form of a travelling wave. As the crystal area (second moment) increases above its steady state value ($\bar{z}_2 = 1.0$), the supersaturation level is reduced below its steady state value resulting in a reduced amount of generated nuclei. As the crystals grow and product is removed from the crystallizer, the crystal area will decrease to below its steady state value due to the previous period of reduced nucleation. This will then lead to increasing supersaturation and an excessive amount

FIGURE 13

TYPICAL CLASSIFIED LIMIT CYCLE

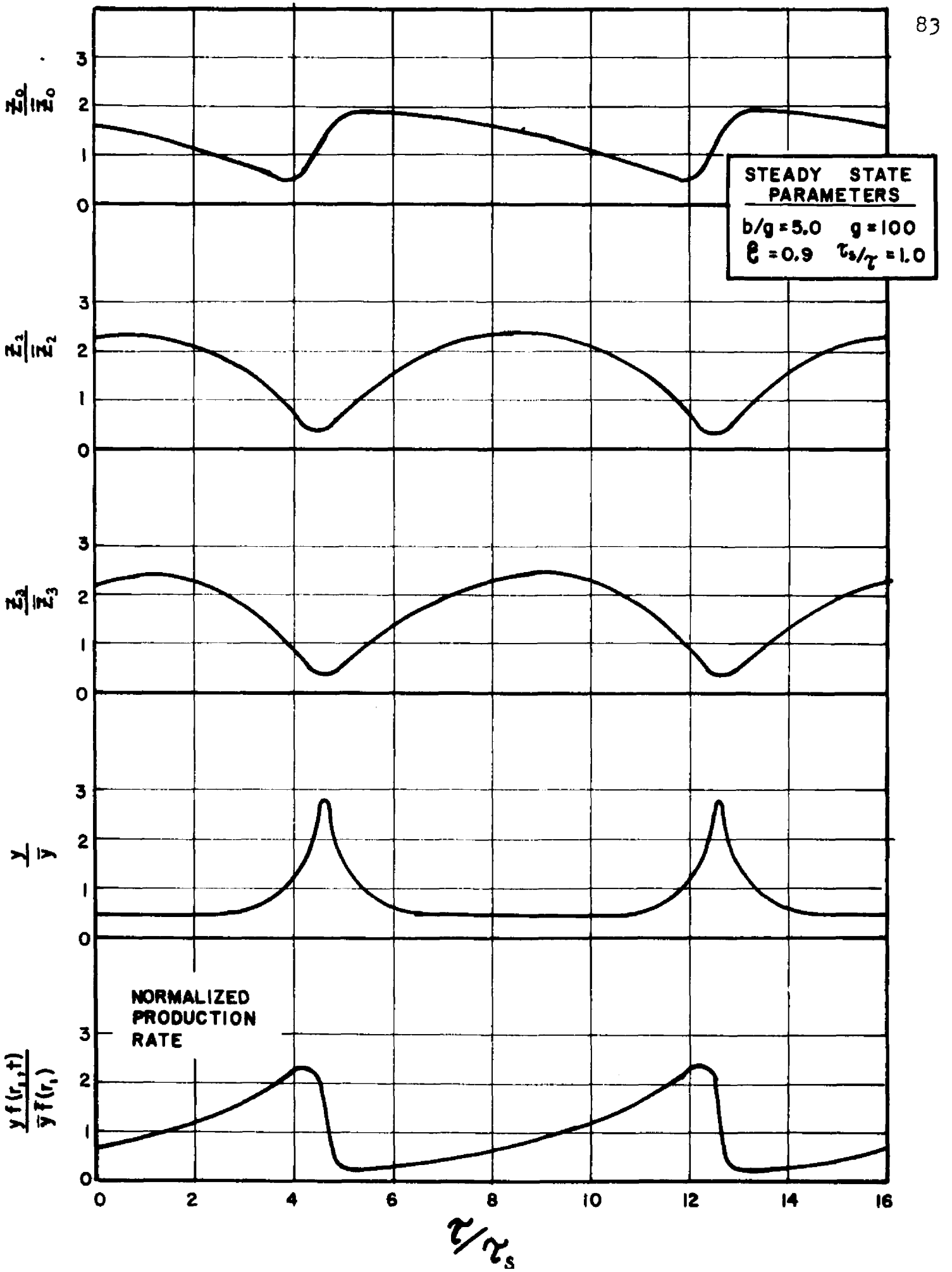

FIGURE 14

PARTICLE DENSITY FLUCTUATIONS OVER A LIMIT CYCLE

STEADY STATE PARAMETERS

$b/g = 5 \quad g = 100 \quad \varepsilon = 0.8 \quad \tau_d/\tau = 1.0$

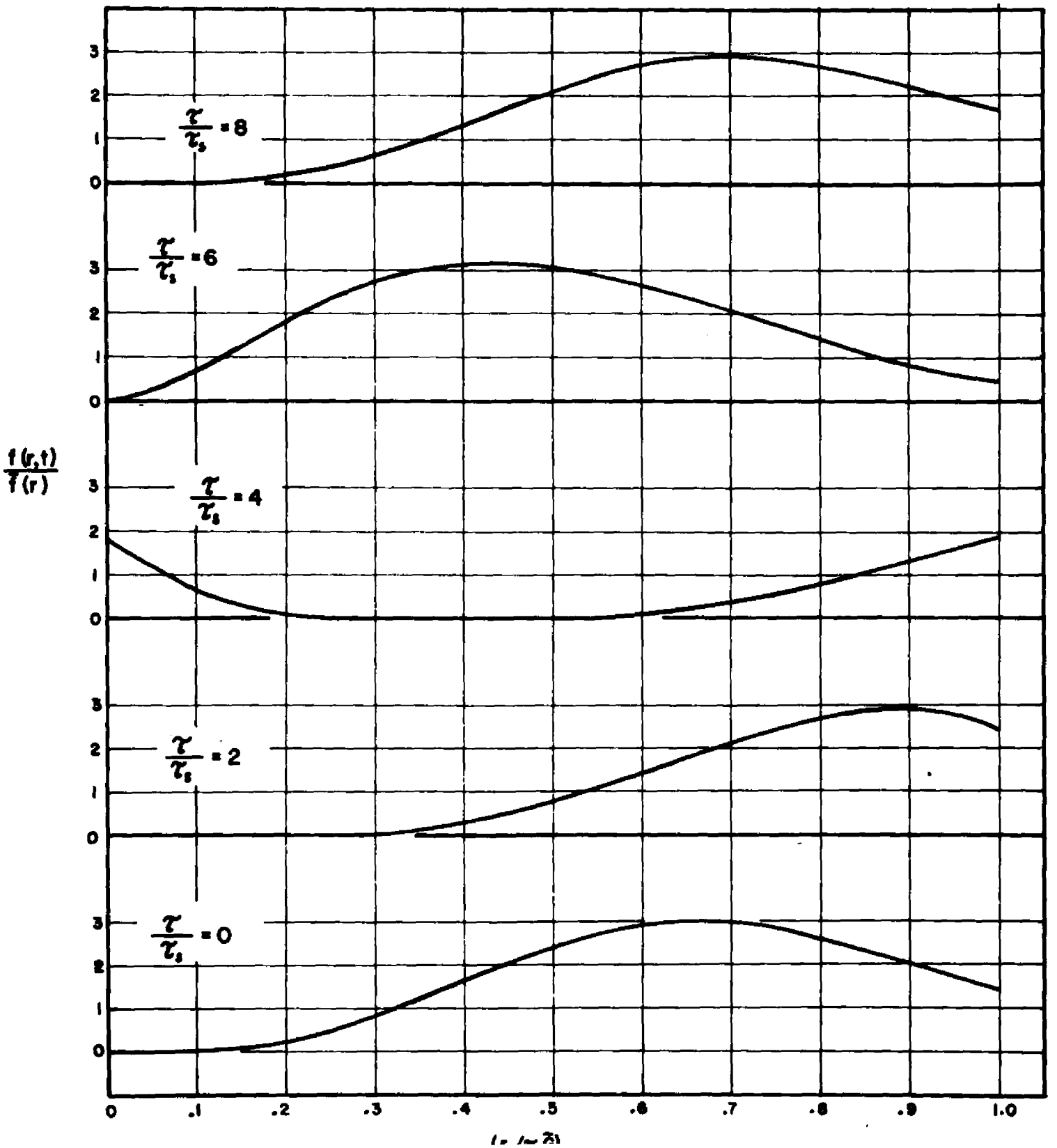

of nucleation. As these nuclei grow to a dominant particle size, the crystal area will increase to greater than steady state values and the cycle will start again.

The limit cycle which results for the classified case is somewhat different from that for non classified operation.

(1) The product is of constant size but the rate of production varies.

(2) The solid content is not constant; the third moment μ_3 fluctuates throughout the cycle and the size of its normalized oscillation is about the same as that for the second moment μ_2 . Also, the second and third moments are in phase with each other.

(3) The cycle time is longer for classified operation than for mixed product removal.

The extent of the oscillations and the cycle time are plotted as a function of b/g in Figure 15 for a particular voidage ($\bar{\epsilon}$ = 0.9). The similarity of the maximum and minimum values of the normalized second and third moments and of the normalized production rate should be noticed. This appears because they are all governed by the particle density near or at the product size r_1 .

FIGURE 15

CLASSIFIED LIMIT CYCLE CHARACTERISTICS AS A FUNCTION OF b/g

$\frac{\tau_p}{\tau} = 1.0 \qquad \bar{\epsilon} = 0.9$

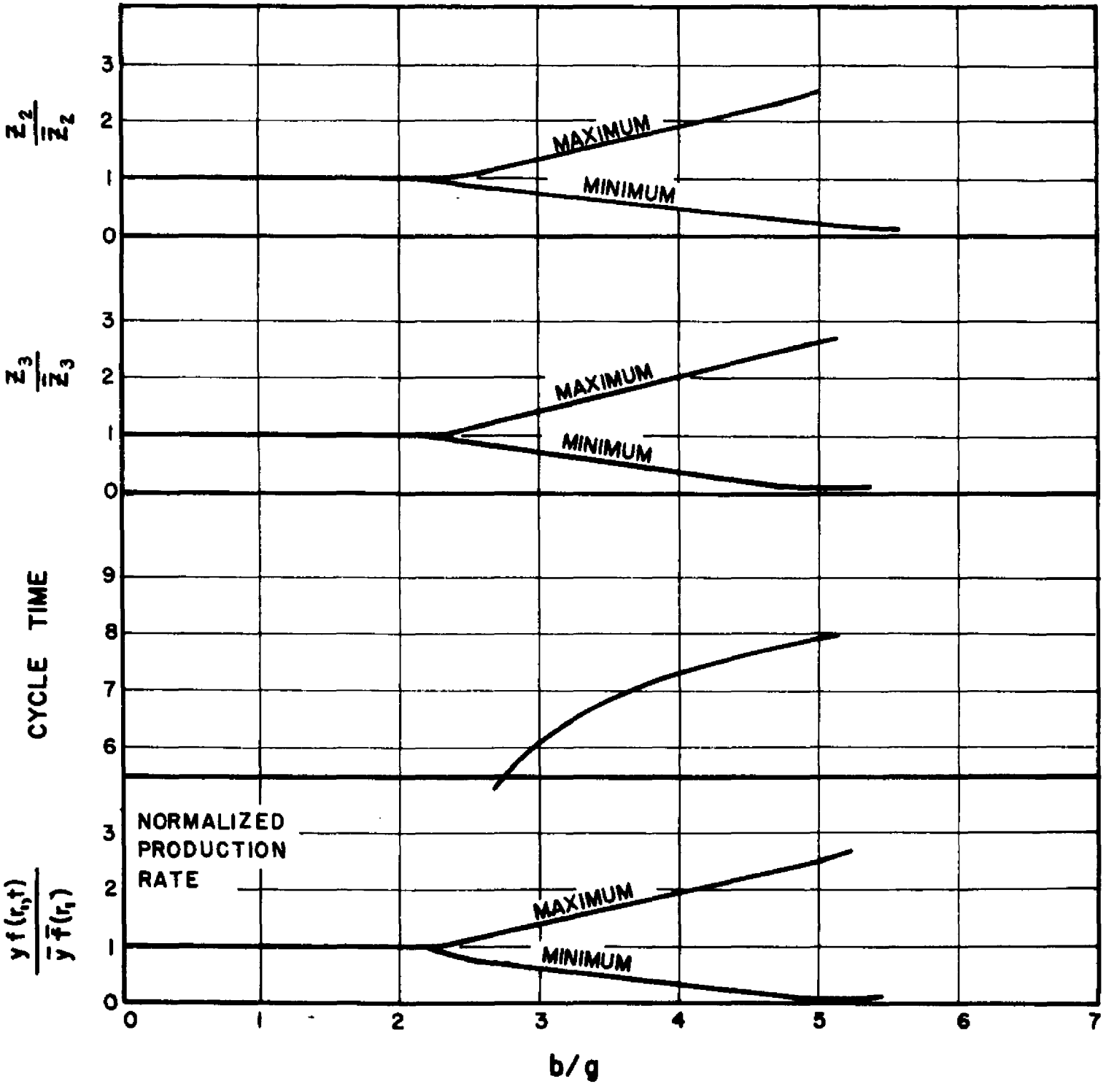

Conclusions

As mentioned in the introduction, it is well established that continuous crystallizers exhibit cycling behavior The occurence of such cycling behavio r is probably much more frequent than most people realize. As shown in the analysis the cycle period is very long, about 3 to 8 times the solids' draw-down time. Such long cycles might therefore involve several operator shifts and the cycle itself might be strongly perturbed or masked by changes introduced by the operator. Depending on the control strategy used by the operator this might enhance instability or just cause an increased variability in the size distribution.

The data available in the literature from which one can calculate values of b/g for a particular system are extremely sparse. However, the two sources which we found both agree with the results of this study.

1. Robinson and Roberts (20) fitted a metastable model to an ammonium sulfate system they were operating in their plant. The plant crystallizer was well stirred and did not classify the product. Utilizing equation (44) and their model, we were able to determine that b/g for this system was greater than 20. Instability and long term transients were reported for this system and to calculate the steady state particle distribution an average of 61 samples were taken over a period of days. According to the results of this thesis, the stability limit for this type of operation is a b/g of about 21 and in all likelihood the instability reported for this

system were the limit cycles predicted by this study. The fact that they obtained a steady state particle balance which fitted steady state theory only by averaging their results over a period of days is also predicted by this thesis, as shown in Figure 9.

2. The study of Bransom (21) with a well stirred isothermal salting out crystallizer provides the best data available in the literature. He studied a cyclonite system with the supersaturation provided by the addition of alcohol. By fitting a modified Volmer model to his data it was found that b/g never exceeded a value of 4.0 for the conditions of his study. Consequently, no cycling problem was reported and a particle size distribution was attained which fit steady state theory without averaging. Residence times were very low for this study (about 15 minutes) and the product crystal was therefore very small. Calculations indicate that if the residence time were increased to about one hour (which would increase the product size), the stability limits would be reached and any attempt to grow still larger crystals would result in cycling.

The analytical treatment given in this paper provides a basis of understanding the general nature of these phenomena. It is seen that the dominating source of this unstable behavior is the strongly non linear nature of the dependence of nucleation rate on supersaturation which, in an oversimplified form, is sometimes described by assuming the existence of a metastable region in which no nucleation occurs. The larger the particle size the lower must be the nucleation rate and therefore for large crystals one has to

operate at supersaturations close to the so-called metastable region. A small upset at these conditions will cause a temporary increase in nucleation rate. Now as the excess amount of nuclei grows the total area increases and the supersaturation decreases, reducing the nucleation rate. However, this effect occurs with a considerable time delay as the new nuclei have no appreciable surface for a considerable time span. Therefore, before the stabilizing action occurs a large number of nuclei might be formed which later will reduce the supersaturation so much that the solution becomes metastable and nucleation practically ceases. At some later time the total surface starts to decrease due to the removal of crystals from the crystallizer in the outflow and the supersaturation starts to increase again.

This leads therefore to the occurence of limit cycles whose specific properties were described in the analytical part and can be summarized as follows:

Both the tendency to instability and the relative amplitude of the limit cycles increase with increasing b/g and therefore with increasing particle size, at otherwise constant conditions.

For the mixed product case:

(1) The free volume or the magma density have little effect on stability.

(2) The cycle period is comparatively long (3 to 5 times the draw-down time).

(3) The instabilities tend to decrease the average particle size and increase the total variance. However, if an individual sample

is withdrawn, chances are quite high that its size distribution will be more uniform than for a Poisson distribution.

(4) Correct feeding of the seed will tend to stabilize the system and increase particle size.

(5) The total crystal mass will in most cases remain almost constant.

For the classified product case:

(1) The magma density can be independently controlled and has a small effect on the stability limits.

(2) The cycle period is longer than for the mixed product case: 6 to 8 times the solid draw-down time.

(3) The instabilities do not effect product size, but do cause cycling in the rate of production.

(4) Simultaneous seeding and increase of the solid volume can stabilize the operation over a wide range of product sizes.

(5) The normalized solid content, crystal area and production rate vary in phase and approximately in magnitude.

At least one remark on the model itself. In all the analysis it was assumed that the crystallizer is an ideally

stirred tank. It should be pointed out in all fairness that for many crystallizers this is not a good approximation. In this model any incoming feed will become immediately dispersed. In reality this takes a finite mixing time varying from a fraction of a second to several seconds, depending on the size of the vessel (mixing time increases with vessel size (14)). Now when using such a model for a regular first or second order chemical reaction with a residence time large as compared to the mixing time the error introduced by neglecting this short initial mixing period is often negligible. In any phenomena involving nucleation the increase in rate of nucleation during this period might be so large that almost all of it will occur during that stage.

One has therefore to be very careful in using such a model in crystallization. In particular it is doubtful if one can calculate nucleation rates from the overall performance of such crystallizers, as has been suggested.

The deviation of an actual mixed crystallizer from that of an ideally mixed one will therefore depend both on the nature of the crystallizing solution and the initial mixing time and therefore the size of the vessel. The latter factor explains some of the special difficulties encountered in the scale-up of crystallizers.

This deviation from ideal mixing will have a similar

effect as seeding and has some stabilizing action. However, even in a case where there are considerable deviations between the actual behaviour of the crystallizer and the ideally mixed theoretical model, the present analysis should still present the correct trends and provides an understanding of the phenomena leading to cyclic behavior of crystallizers.

6. Appendices

Appendix 6.1

Stability Analysis - Clear Feed

The characteristic set of linearized equations is given by the left side of (48) and the steady state groups Ln and Rn by (46) and (47).

Taking the LaPlace transform of this set of equations and defining:

$$T_n = [L_n(\theta - b) + b] \qquad n = 0, 1, 2, 3 \ldots$$

the denominator of any Transfer Function (the Characteristic Matrix) can be written as:

Variable → / equation ↓	$\hat{z}_0'(s)$	$\hat{z}_1'(s)$	$\hat{z}_2'(s)$	$\hat{z}_3'(s)$	$Y'(s)$
0 moment	(S+1)	0	0	Ro	-To
1 moment	$-L_1$	(S+1)	0	R_1	$-T_1$
2 moment	0	-L2	(S+1)	R2	-T2
3 moment	0	0	$-L_3$	$(S+1+R_3)$	$-T_3$
Conc. Balance	0	0	$+L_3$	$-R_3$	$(S+1+T_3)$

This can be expanded to give the characteristic fifth order equation:

$$a_5 S^5 + a_4 S^4 + a_3 S^3 + a_2 S^2 + a_1 S + a_0 = 0$$

where $a_5 = 1.$

$$a_4 = 5 + (R_3 + T_3)$$

$$a_3 = 10 + 4(R_3 + T_3) + [L_3(R_2 + T_2) - R_3 T_3]$$

$$a_2 = 10 + 6(R_3 + T_3) + 3[L_3(R_2 + T_2) - R_3 T_3] + L_2 L_3 (R_1 + T_1)$$

$$a_1 = 5 + 4(R_3 + T_3) + 3[L_3(R_2 + T_2) - R_3 T_3] + 2L_2 L_3 (R_1 + T_1) + 4 L_2 L_3 (R_0 + T_0)$$

$$a_0 = 1 + (R_3 + T_3) + [L_3(R_2 + T_2) - R_3 T_3] + L_2 L_3 (R_1 + T_1) + L_1 L_2 L_3 (R_0 + T_0)$$

Using the form of Routh's criterion given in Wylie, "Advanced Mathematics for Engineers", a root will be in the right hand S plane (hence unstable) whenever any one of the determinants are not positive. (This assumes that all the coefficients a_n are positive).

$$|a_4| > 0$$

$$\begin{vmatrix} a_4 & a_5 \\ a_3 & a_4 \end{vmatrix} > 0$$

$$\begin{vmatrix} a_4 & a_5 & 0 \\ a_3 & a_4 & a_5 \\ a_2 & a_3 & a_4 \end{vmatrix} > 0$$

$$\begin{vmatrix} a_4 & a_5 & 0 & 0 \\ a_3 & a_4 & a_5 & 0 \\ a_2 & a_3 & a_4 & a_5 \\ a_1 & a_2 & a_3 & a_4 \end{vmatrix} > 0$$

$$\begin{vmatrix} a_4 & a_5 & 0 & 0 & 0 \\ a_3 & a_4 & a_5 & 0 & 0 \\ a_2 & a_3 & a_4 & a_5 & 0 \\ a_1 & a_2 & a_3 & a_4 & a_5 \\ a_0 & a_1 & a_2 & a_3 & a_4 \end{vmatrix} > 0$$

The calculations were carried out with the aid of a digital computer. It should be mentioned that the fourth order determinant was the one which first became negative.

Appendix 6.2

Stability Analysis - Effect of Seed Addition

Substituting definitons (35), (36) and (37) into (34) and defining:

$$T_n = \left[L_n (q - b) + (1 - S_n) b \right]$$

the linearized set of equations becomes:

$$\frac{dZ_n'}{d\theta} - T_n Y' - L_n Z_{n-1}' + R_n Z_3' + Z_n' = f(\theta)(S_{n-1}) \qquad n = 0, 1, 2, 3 \ldots$$

$$\frac{dY'}{d\theta} + T_3 Y' + Y' + L_3 Z_2' - R_3 Z_3' = f(\theta) \frac{\bar{\varepsilon}_0 - \bar{\varepsilon}}{1 - \bar{\varepsilon}}$$

To determine the effect of seed size and number, we let the generated nuclei size equal zero ($\alpha = 0$) such that R_1, R_2 and R_3 are zero.

Taking the LaPlace transform of the above set of equations, the denominator of any Transfer Function (the Characteristic Matrix) can be written:

Variable → / equation ↓	$\hat{Z}_0'(s)$	$\hat{Z}_1'(s)$	$\hat{Z}_2'(s)$	$\hat{Z}_3'(s)$	$\hat{Y}'(s)$
0 moment	(S+1)	0	0	Ro	-To
1 moment	$-L_1$	(S+1)	0	0	$-T_1$
2 moment	0	$-L_2$	(S+1)	0	$-T_2$
3 moment	0	0	$-L_3$	(S+1)	$-T_3$
Conc. Balance	0	0	$+L_3$	0	$(S+1+T_3)$

Comparing this Matrix with the clear feed case, it is apparent that the coefficients of the expanded fifth order characteristic equation can be calculated from the results of the clear feed calculations (just set R_1, R_2 and R_3 equal to 0).

The procedure for determining stability is exactly the same as was previously discussed.

The difference between the seeded and clear feed case is in the determination of the steady state parameters Ln, Rn, Sn and in the definition of Tn.

For the assumption that the seed distribution is a delta function and using relations (53-56) we can calculate:

$$L_1 = (1+\Sigma)/(1+\Sigma(\beta+1))$$

$$L_2 = 2(1+\Sigma(\beta+1))/(2+\Sigma(\beta^2+2\beta+2))$$

$$L_3 = 3(2+\Sigma(\beta^2+2\beta+2))/(6+\Sigma(\beta^3+3\beta^2+6\beta+6))$$

$$R_0 = \frac{1-\bar{\epsilon}}{\bar{\epsilon}}\,\frac{1}{1+\Sigma}$$

$$S_0 = \Sigma/(1+\Sigma)$$

$$S_1 = \beta\Sigma/(1+\Sigma(\beta+1))$$

$$S_2 = \beta^2\Sigma/(2+\Sigma(\beta^2+2\beta+1))$$

$$S_3 = \beta^3\Sigma/(6+\Sigma(\beta^3+3\beta^2+6\beta+6))$$

Appendix 6.3

Stability Analysis - Effect of Size Dependent Growth Model

In order to estimate the effect of size dependent growth rates, we approximate $\frac{dr}{dt}$ by:

$$\frac{dr}{dt} = G(c)\phi(r) = G(c)(1+ar)$$

When this is done equations (20) and (11) give the following set of equations:

$$\frac{d\mu_n}{dt} = nG(\mu_{n-1} + a\mu_n) + (1-K\mu_3)B(c)r_0^n + \frac{\omega}{V}\gamma_n - \frac{\omega}{V}\mu_n \qquad n=0,1,2,3\ldots$$

$$(1-K\mu_3)\frac{dc}{dt} = \frac{\omega}{V}(c_0-c)(1-K\gamma_3) - (\rho-c)[3KG(\mu_2+a\mu_3)+(1-K\mu_3)BKr_0^3]$$

By linearizing these equations and utilizing the definitions given by equations (27-33) and (35-37) plus the definition of a new steady state group:

$$M = \frac{V}{\omega}Ga$$

we get the following linearized and normalized equations:

$$\frac{dZ_n'}{d\theta} - [(L_n+nM)q + b - S_n b - (L_n+nM)b]Y' - L_n Z_{n-1}' + R_n Z_3' + (1-nM)Z_n' = f(\theta)(S_n-1) \qquad n=0,1,2,3\ldots$$

$$\frac{dY'}{d\theta} + [(L_3+3M)q + b - S_3 b - (L_3+3M)b]Y' + Y' + L_3 Z_2' + [3M-R_3]Z_2' = f(\theta)\frac{\bar{E}_0-\bar{E}}{1-\bar{E}}$$

Let us now disregard the seed terms for this study. (For a clear feed Sn = 0). Let us also take the nuclei size equal to zero here (α = 0; R_1 , R_2 and R_3 = 0).

If we then define Tn such that

$$T_n = \left[(L_n + nM)(q-b) + b \right]$$

and take the LaPlace Transform of the linearized set, we get the following Characteristic Matrix:

Variable → / equation ↓	$\hat{z}_0'(s)$	$\hat{z}_1'(s)$	$\hat{z}_2'(s)$	$\hat{z}_3'(s)$	$\hat{y}'(s)$
0 moments	(S+1)	0	0	Ro	-To
1 moments	$-L_1$	(S+1-M)	0	0	$-T_1$
2 moments	0	$-L_2$	(S+1-2M)	0	$-T_2$
3 moments	0	0	$-L_3$	(S+1-3M)	$-T_3$
Conc. Bal.	0	0	$+L_3$	3M	(S+1+T_3)

This can be expanded to give the characteristic fifth order equations:

$$a_5 S^5 + a_4 S^4 + a_3 S^3 + a_2 S^2 + a_1 S + a_0 = 0$$

where: $a_5 = 1.$

$$a_4 = 5 + T_3 - 6M$$

$$a_3 = 10. + 4T_3 + T_2 L_3 - M(3T_3 + 24) + 11M^2$$

$$a_2 = 10 + 6T_3 + 3T_2L_3 + T_1L_2L_3 - M(36 + 9T_3 + T_2L_3) + M^2(33 + 4T_3) - 6M^3$$

$$a_1 = 5 + 4T_3 + 3T_2L_3 + 2T_1L_2L_3 + L_1L_2L_3(R_0 + T_1) - M(24 + 9T_3 + 2T_2L_3) + M^2(33 + 4T_3) - 12M^3$$

$$a_0 = 1 + T_3T_2L_3 + T_1L_2L_3 + L_1L_2L_3(R_0 + T_0) - M(6 + 3T_3 + T_2L_3) + M^2(11 + 2T_3) - 6M^3$$

To determine the stability of the system we again used Routh's criterion as outlined for the clear feed case.

The problem arising when studying this effect is that the steady state distribution and moments differ from the case where $\phi = 1$.

From the steady state particle balance we find:

$$\bar{f}(r) = \frac{\bar{\varepsilon}\bar{B}}{\bar{G}} \frac{(1+ar_0)^{\frac{w}{VG}\frac{1}{a}}}{(1+ar)^{(\frac{w}{VG}\frac{1}{a}+1)}} = \frac{\bar{\varepsilon}\bar{B}}{\bar{G}} \frac{1}{(1+ar)^{(1+1/n)}} \quad \text{when } r_0 = 0$$

or

$$\bar{f}(r) = \frac{\bar{\varepsilon}\bar{B}}{\bar{G}(1+ar)} e^{-\frac{w}{V}\int_{r_0}^{r} \frac{dy}{\bar{G}(1+ay)}}$$

Integrating the moments from the above, and for each moment n assuming the term $M < \frac{1}{n}$ (which coincides with the assumption of investigating a first order correction), we get:

$$M_0 = \bar{\varepsilon}\bar{B} / wN$$

$$\mu_1 = \bar{E}\bar{B}/[\omega_v(\tfrac{1}{M}-1)a]$$

$$\mu_2 = 2\bar{E}\bar{B}/[\tfrac{\omega}{v}(\tfrac{1}{M}-1)(\tfrac{1}{M}-2)a]$$

$$\mu_3 = 6\bar{E}\bar{B}/[\tfrac{\omega}{v}(\tfrac{1}{M}-1)(\tfrac{1}{M}-2)(\tfrac{1}{M}-3)a]$$

These moments can then be substituted into (35) and (36) to calculate Ln, n = 1, 2, 3 and R_o.

Appendix 6.4

Operation with and without a fines trap to produce the same product; a comparison of stability:

In the following, let all parameters related to operation with a fines trap be denoted by a subscript f.

The nucleation rates for the two modes of operation can be written as follows, using equations (40) and (61), and assuming C/C_s is close to 1.

$$\mathcal{B}_f = k_2 e^{-\frac{K_3}{\left(\frac{C}{C_s}-1\right)^2}} e^{-\frac{r_c}{\tau' G_f}} \qquad (a)$$

$$\mathcal{B} = k_2 e^{-\frac{K_3}{\left(\frac{C}{C_s}-1\right)^2}} \qquad (b)$$

Assuming a linear growth model (equation 38) the sensitivity parameter b/g for the two modes of operation can be evaluated as described in equations (62) and (63):

$$\left(\frac{b}{g}\right)^*_f = \frac{2K_3 C_s^2}{(C-C_s)^2} + \frac{r_c}{\tau' G_f} = \left(\frac{b}{g}\right)_f + \frac{r_c}{\tau' G_f} \qquad (c)$$

$$\left(\frac{b}{g}\right)^* = \frac{2K_3 C_s^2}{(C-C_s)^2} = \frac{b}{g} \qquad (d)$$

Now in order for the product to be the same for the two modes of operation we require the Weight Mean Size $\bar{\mu}_4/\bar{\mu}_3$ to be the same. From equations (25-unseeded) this yields:

$$\tau_f G_f = \tau G \qquad (e)$$

The similarity condition also requires the nucleation rate to be proportional to the feed rate or inversely proportional to the residence time so that:

$$\frac{B_f}{B} = \frac{\tau}{\tau_f} \tag{f}$$

and combining (e) and (f):

$$\frac{B_f}{G_f} = \frac{B}{G} \tag{g}$$

Now taking the ratio (b/g)f and (b/g) from (c) and (d) gives:

$$\frac{(b/g)^*_f}{(b/g)} = \frac{(C-C_s)^2}{(C_f-C_s)^2} + \frac{\frac{r_c}{\tau' G_f}}{(b/g)} \tag{h}$$

From equation (38) it can be seen that:

$$\frac{(C-C_s)^2}{(C_f-C_s)^2} = \left(\frac{G}{G_f}\right)^2 \tag{i}$$

so that substitution of (i) and then (g) into (h) yields:

$$\frac{(b/g)^*_f}{(b/g)} = \left(\frac{B}{B_f}\right)^2 + \frac{\frac{r_c}{\tau' G_f}}{(b/g)} \tag{j}$$

Substitution of (a) and (b) into (j) results in:

$$\frac{(b/g)^*_f}{(b/g)} = e^{\left[\frac{(b/g)_f}{b/g} + \frac{r_c}{\tau' G_f}\frac{1}{b/g} - 1\right]\frac{b}{g}} + \frac{\frac{r_c}{\tau' G_f}}{b/g} \tag{k}$$

We now wish to know if, with realistic values for $r_c/t'G_f$ and (b/g), the ratio (b/g)*f/(b/g) will depart greatly from one. Values of this ratio greater than one indicate a decreasing stability while values less than one indicate the opposite.

Values for $r_c/t'G_f$ of 1.0 and 2.38 refer to 67% and 91% fines removal respectively. Assuming the initial system is at the stability borderline (b/g near 20), the term $(r_c/t'G_f)/(b/g)$ would have a value in the range of .05 to 0.10 for the fines removal rates indicated above. With these values equation (K) can be solved and it is found that the ratio (b/g)*f/(b/g) is slightly smaller than one, indicating the addition of a fines trap will not itself cause instability.

Appendix 6.5

Non Linear Solutions to the Mixed Product Model

The normalized system equations used are given by equations (73), (74) and (75). They are ordinary non linear differential equations and were solved numerically by use of the Runga-Kutta-Gill technique.*

When solving these equations with (b/g) value of 15 and higher a time step size of 0.002 or smaller will result in a convergent solution. It is probably possible to take larger steps and just reduce the step size when the relative supersaturation level starts to rise but this was not done here.

*Mathematical Methods for Digital Computers by A. Ralston and H. Wilf, Wiley, 1959 - pp. 110-121.

Appendix 6.6

Relation of the cycle average Coefficient of Variation to the steady state value:

This relation is derived for the case when $\alpha = 0$ and the feed is clear. For a crystallizer, the supersaturation is so small that μ_3 or ε is taken as a constant.

Steady State

$$\bar{\gamma}^2 = \frac{\frac{\bar{\mu}_5}{\bar{\mu}_3} - \left(\frac{\bar{\mu}_4}{\bar{\mu}_3}\right)^2}{\left(\frac{\bar{\mu}_4}{\bar{\mu}_3}\right)^2} = \frac{\bar{\mu}_3 \bar{\mu}_5}{\bar{\mu}_4^2} - 1$$

Substituting the relations of (15) for the steady state moments gives:

$$\bar{\gamma}^2 = \frac{5}{4} - 1 = \frac{1}{4} \qquad \text{(a)}$$

$$\bar{\gamma} = 0.5$$

Calculation will show that even for values of $\alpha = 0.1$, the steady state Coefficient of Variation will still be 0.5.

Limit Cycle Average

The average of a moment taken over a limit cycle of time θ can be written:

$$\{\mu_n\} = \frac{1}{\theta}\int_{\tau}^{\tau+\theta} \mu_n \, dt$$

In order to get a composite value for the Coefficient

of Variation over the limit cycle, the cycle average Variance should be evaluated with respect to the cycle average weight mean size.

$$\{\gamma^2\} = \frac{\frac{\{\mu_5\}}{\mu_3} - \frac{\{\mu_4\}^2}{\mu_3^2}}{\frac{\{\mu_4\}^2}{\mu_3^2}} \qquad \text{(b)}$$

When $r_o = 0$ and the feed is clear, the moment equations for μ_4 and μ_5 can be written from (12) as:

$$\frac{d\mu_4}{dt} = 4G\mu_3 - \frac{\omega}{V}\mu_4 \qquad \text{(c)}$$

$$\frac{d\mu_5}{dt} = 5G\mu_4 - \frac{\omega}{V}\mu_5 \qquad \text{(d)}$$

When a periodic solution is assumed for μ_n, integration of these equations over a cycle givesn for (d):

$$\int_t^{t+\theta} \frac{d\mu_5}{dt}\,dt = \mu_5\Big|_t^{t+\theta} = 0 = 5\theta\{G\mu_4\} - \frac{\omega}{V}\theta\{\mu_5\} \qquad \text{(e)}$$

$$\{\mu_5\} = 5\frac{V}{\omega}\{G\mu_4\}$$

Substituting this into (b):

$$\{\gamma^2\} = \frac{5\frac{V}{\omega}\mu_3\{G\mu_4\}}{\{\mu_4\}^2} - 1 \qquad \text{(f)}$$

Multiplying (c) by μ_4 and integrating over the cycle:

$$\mu_4 \frac{d\mu_4}{dt} = \frac{1}{2}\frac{d\mu_4^2}{dt} = 4G\mu_3\mu_4 - \frac{\omega}{V}\mu_4^2$$

$$\frac{1}{2}\int_t^{t+\theta} \frac{d\mu_4^2}{dt}dt = 0 = 4\mu_3\{G\mu_4\} - \frac{\omega}{V}\{\mu_4^2\}$$

$$\{G\mu_4\} = \frac{\frac{\omega}{V}\{\mu_4^2\}}{4\mu_3} \qquad (g)$$

and substituting (g) into (f):

$$\{\gamma^2\} = 5\frac{\{\mu_4^2\}}{\{\mu_4\}} - 1 \qquad (h)$$

Substracting the steady state $\bar{\gamma}^2$ from $\{\gamma^2\}$

$$\{\gamma^2\} - \bar{\gamma}^2 = \frac{5}{4}\left[\frac{\{\mu_4^2\}}{\{\mu_4\}^2} - 1\right]$$

The term in parenthesis is the Coefficient of Variation of μ_4 and since $\{\mu_4^2\} \geq \{\mu_4\}^2$, it is apparent that the accumulated product from a limit cycle will not be tighter than the product from steady state operation. Generally, μ_4 does not fluctuate very much and, therefore, the cycle average $\{\gamma\}$ will be close to the steady state value of 0.5 as shown in Figure 6.

Appendix 6.7

Stabilization by Seeding

Initial (unstable) conditions are denoted here by a subscript i.

Assumptions:

1. $\alpha = \gamma_0 = 0$.
2. $G = K_1(C - C_s)$
3. $B = K_2 e^{-\frac{C_s^2 K_3}{(C-C_s)^2}}$ (Volmer Model)

so $$\left(\frac{b}{g}\right)^* = \frac{2K_3 C_s^2}{(C-C_s)^2} = \frac{K_4}{(C-C_s)^2} = \frac{b}{g}$$

4. τ and C_s are constant

Independent Variables:

1. Seed size $\beta' = \frac{r_s}{\tau G_i}$ (based on initial conditions)

$$\beta = \frac{r_s}{\tau} = \beta' \frac{G_i}{G} \qquad (a)$$

2. S ; from which we can calculate (See Appendix 6.2)

$$S_3 = \frac{1-\varepsilon_0}{1-\varepsilon} = \frac{\beta^3 S}{6 + S(\beta^3 + 3\beta^2 + 6\beta + 6)} \qquad (b)$$

Relations:

By equation τ's from the two steady state mass balances, we can show

$$\varepsilon_0 G_i \mu_{2i} = G \mu_2$$

Substituting from (56) for μ_2 and μ_{2i} $(\delta+\beta=0)$ above and noting that:

$$\varepsilon = \varepsilon_i \varepsilon_0 \qquad (c)$$

and using relations (108) and (109), we get:

$$e^{\frac{1}{2}\left(\frac{b}{q}\right)_i}\left(\frac{b}{q}\right)_i^{\frac{3}{2}} = e^{\frac{1}{2}\left(\frac{b}{q}\right)}\left(\frac{b}{q}\right)^{\frac{3}{2}}\frac{2}{2+\delta(\beta^2+2\beta+2)} \qquad (d)$$

Now using relations (a), (b), (c), (d) and (108) and (109) and our previously derived stability criterion, we performed a trial and error calculation to find the combination of seed size and quantity which would stabilize a given system.

Appendix 6.8

Stability Analysis - Classified Product Case

The characteristic matrix for this case is given by equation (103)and the denominator of any transfer function will have the following form:

$$A_5 S^5+A_4 S^4+A_3 S^3+A_2 S^2+A_1 S+A_0+e^{-4S}(B_4 S^4+B_3 S^3+B_2 S^2+B_1 S+B_0)$$

If we let

$$N=(1-\bar{\varepsilon})/\bar{\varepsilon}$$

$$C=(b-g)$$

$$P=g+[\tau_3/\tau-(1-\bar{\varepsilon})]/\bar{\varepsilon}$$

these coefficients work out to be:

$A_5 = 1.$

$A_4 = P$ $\qquad B_4 = -N$

$A_3 = 0$ $\qquad B_3 = -PN - \frac{3}{4}(N+C)$

$A_2 = 0$ $\qquad B_2 = -\frac{3}{4}NP - \frac{3}{8}(N+C)$

$A_1 = \frac{3}{32}(N+C)$ $\qquad B_1 = -\frac{3}{8}NP - \frac{3}{32}(N+C)$

$A_0 = \frac{3}{32}NP$ $\qquad B_0 = -\frac{3}{32}NP$

Nyquist Diagrams

At first we attempted to work with only the denominator of the transfer function. It was found that when this was done the number of roots on the real side of the S plane was always 2 more than an actual solution for the roots indicated.

We found that this was due to the fact that a

factor of S^4 should have been cancelled from the numerator and denominator. This becomes apparent if e^{-4S} is expanded in a power series:

$$e^{-4S} = 1 - 4S + \frac{(4S)^2}{2!} - \frac{(4S)^3}{3!} + \cdots$$

and the coefficients of a new polynomial of the form

$$P = C_n S^n + C_{n-1} S^{n-1} + \cdots C_1 S + C_0$$

are evaluated. The first four terms C_0, C_1, C_2 and C_3 are identically zero in both the numerator and denominator of any transfer function (This was not true when $r_0 \neq 0$).

When taking this into account the contribution to the rotation of the argument when integrating over the infinite semicircle will come out to be π instead of 5π which results when S^4 is not cancelled.

The drawing of a Nyquist diagram for a transfer function containing transcendental terms results in a curve containing many loops, most of which do not contribute to the angular variation. An example of some typical results are shown below for the following parameters:

$b/g = 3$ $\quad \bar{\varepsilon} = 0.9$ $\quad g = 500$ $\quad \tau_s/\tau = 1.0$

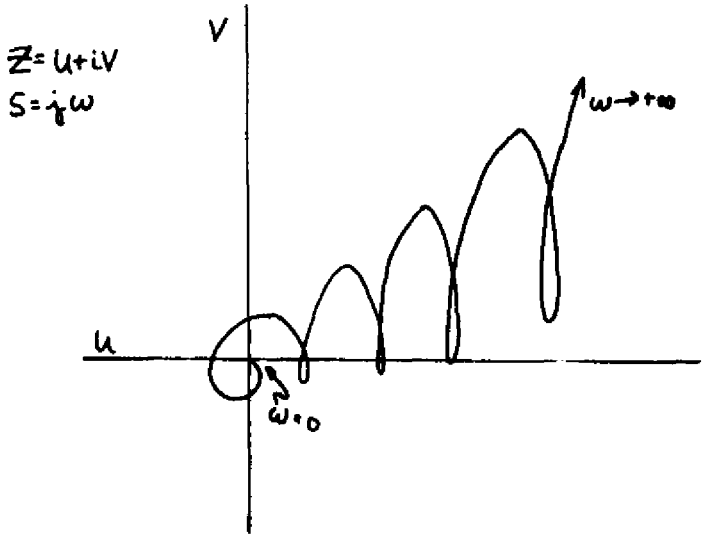

Angular rotation along $j\omega$ axis $+\infty$ to $-\infty$	$+3\pi$
along semicircle	π
Total	4π
No roots in right hand plane	2

The number of roots will always be multiples of two unless there are roots which lie on the real axis of the S plane.

Crossover Points

If in equation (104) we allow $S=j\omega$, expansion of the terms results in an expression for which both the real and complex terms equal zero:

$$j\{A_5\omega^5 - A_3\omega^3 + A_1\omega - [\cos(4\omega)]B_3\omega^3 + [\cos(4\omega)]B_1\omega - [\sin(4\omega)]B_4\omega^4 + [\sin(4\omega)]B_2\omega^2 - [\sin(4\omega)]B_0\} = 0$$

$$\{A_4\omega^4 - A_2\omega^2 + A_0 + [\cos(4\omega)]B_4\omega^4 - [\cos(4\omega)]B_2\omega^2 + [\cos(4\omega)]B_0 - [\sin(4\omega)]B_3\omega^3 + [\sin(4\omega)]B_1\omega\} = 0$$

If we fix all the steady state parameters except b/g, we can numerically investigate the b/g-ω plane to determine at what points the above equations hold. Only

positive values for b/g and ω need be considered. Solutions to these equations will indicate that at these specific steady state values a root will lie on the imaginary axis at $+j\omega$ for the particular value of b/g. Then this root will either lie to the left (stable) of the imaginary axis or to the right of the imaginary axis (unstable) for lower or upper values of b/g. In other words we know this is a crossover point for the root but this treatment will not tell us in which direction the root is travelling with changes in b/g.

This type of study results in a series of harmonic solutions for b/g and ω .

For instance, at the steady state parameters

$\bar{\zeta} = 0.9 \qquad g = 100 \qquad \tau_t/\tau = 1.0$

the following crossover points were found:

b/g	ω
2.3	1.0
4.8	1.7
7.0	4.3

To determine the number of roots in right hand plane in the regions of b/g

0 - 2.3

2.3 - 4.8

4.8 - 7.0

it was necessary to specify the steady state parameters including b/g and to let $s = u + i\omega$ in equation (104). This again will lead to two equations, both equalling zero.

Then the u-ν plane is searched numerically to locate the poles. For the above case it was there were no roots in the right hand plane for values of b/g less than 2.3. There were two roots in the right hand plane for values of b/g between 2.3 and 4.8 and four roots for values between 4.8 and 7.0. From this study it became obvious that the lowest crossover point was the stability limit for the system.

Appendix 6.9

Non Linear Solutions to the Classified Product Model

The normalized system model is given in the set of equations (125).

The method of solution used was to decompose the partial differential equation for $\mathcal{F}(l,\theta)$ into a finite number of ordinary differential equations by approximating the partial $\frac{\partial \mathcal{F}}{\partial l}$ by a finite difference $\frac{\mathcal{F}_i - \mathcal{F}_{i-1}}{l_i - l_{i-1}}$. If the spacing along the l coordinate is broken into n spaces equally, such that each portion covers a distance $1.0/n$ equal to Δ , the normalized particle balance over each portion can be approximated by:

$$\frac{d\mathcal{F}_i}{d\theta} + \frac{\gamma}{4}\frac{\mathcal{F}_i - \mathcal{F}_{i-1}}{\Delta} = 0$$

The moments were calculated from the values of $\mathcal{F}_i$, by assuming it varies linearly between successive points. A three point approximation, such as Sterling's formula would have been better, but the l axis was divided into enough sections so that the two point linear approximation was satisfactory. The moment equation can be approximated by:

$$Z_n = \sum_{i=1}^{k} \left[\frac{\mathcal{F}_i - \mathcal{F}_{i-1}}{\Delta} \left\{ \frac{n+1}{n+2}\left(l_i^{n+2} - l_{i-1}^{n+2}\right) - l_{i-1}\left(l_i^{n+1} - l_{i-1}^{n+1}\right) \right\} + \gamma_{i-1}\left(l_i^{n+1} - l_{i-1}^{n+1}\right) \right]$$

Having reduced the partial differential for the

normalixed particle balance to a number of ordinary differential equations, we combined it with the concentration balance and used a Runga-Kutta-Gill routine to calculate the solutions.

It was found that decomposing the l axis to twenty subdivisions was sufficient to get a convergent solution. The time step used in the Runga-Kutta-Gill subroutine must be kept below 0.01 to get a convergent solution. In addition, whenever the relative supersaturation (Y) exceeded 1.5 the time step should be reduced to 0.002 to insure convergence.

The decomposition of the position and time axes cannot be done individually since stability problems similar to those described for the classical diffusion equation will arise. It is estimated from computational experience that the term $\frac{Y(\theta_i-\theta_{i-1})}{l_i-l_{i-1}}$ should not exceed 0.10 to 0.15.

It is also recommended to include a test in the program to insure that values for $\mathcal{F}_i$ are not less than zero. This problem can arise when values for b/g are equal to 5 or more, and supersaturation fluctuations are large enough to reduce the nucleation rate to approximately zero at times.

7. Nomenclature

a - constant is size dependent growth model - equat. 39

b - dimensionless nucleation sensitivity group

$\frac{b^*}{g}$ - system sensitivity parameter

B^0 - nucleation rate per volume of solution

c - solute concentration in the crystallizer

c_o - solute concentration in the feed

c_n - metastable concentration

c_s - solubility concentration of the solute

$f(r,t)dr$ - number of crystals per unit volume having radii in the range r, r + dr at time t

$f'(r,t)$ - crystal density perturbation

$\mathcal{F}(r,t)$ - normalized crystal density $f/\mathcal{F}$

$\mathcal{F}'(r,t)$ - normalized crystal density perturbation

$F(t)$ - fraction of particles residing in a vessel for a period of time less than τ

g - dimensionless growth sensitivity group

$G(c)$ - crystal growth rate dependence on concentration

$h(\theta)$ - normalized feed concentration

$j(\theta)$ - normalized feed rate

K - crystal shape factor

K_n - constants

l - classified case, normalized crystal size r/r_1

L_n - steady state dimensionless groups dependent on α

m - exponent in metastable nucleation function

$p(\theta)$ - dimensionless feed rate for stability analysis

$g(\theta)$ - dimensionless feed concentration for stability analysis

r - characteristic radius of the crystal

r_c - nuclei trap cutoff size

r_o - nuclei characteristic radius

r_s - seed size

r_{WM} - mean particle size with regard to the weight distribution

r_i - product size for the classified product crystallizer

R_n - steady state dimensionless groups dependent on $\bar{\varepsilon}$ and α

t - time

$\bar{v}$ - partial molar volume of solute

V - crystallizer working volume

$W_r dr$ - crystal weight per volume having radii in the range r, r + dr

Y - normalized supersaturation

Y' - dimensionless concentration perturbation

Z_n - normalized moments

Z_n' - dimensionless moment perturbations

η_n - nth moment of ψ

Greek Letters

α - dimension group defined in equation (25) $r_o/\tau G$

β - dimension group defined in equation (32) $G/\tau G$

γ - coefficient of variation

ε - fractional volume of solution

ε_p - fractional volume of solution in the outlet of a classified product crystallizer

ζ - ratio of seed rate to nucleation

θ - dimensionless time

μ_n - nth moment of f(r)

ρ - crystal density

τ - crystallizer draw-down time V/ω

τ' - draw-down time based on flow to the nuclei trap

ϕ - crystal growth rate dependence on r

$\psi(r,t)dr$ - number of crystals per volume of feed having radii in the range r, r + dr, at time t

ω - volumetric feed and/or withdrawal rate

Subscripts

o - properties of feed

1 - properties of take off

c - classified operation

M - mixed production operation

Superscripts

$\bar{}$ - steady state values

$'$ - perturbation from steady state

$\wedge$ - LaPlace Transform

8. References

1. Aris R. & Amundson N.R., Chem. Eng. Science, 7, No. 3, 121 (1958), Parts 1, 2 & 3.

2. Bransom, S.H., British Chemical Eng., 838 (1960).

3. Cannon K.J. & Amundson N.R., A.I.Ch.E. Journal, 9, 297 (1963).

4. Crocco N. & Cheng S., "Rocket Instability", Butterworths, (1956).

5. Finn & Wilson, Agricultural & Food Chemistry, 2, No. 2, 66 (1954).

6. Han C.D. & Shinnar R., Paper submitted to the 60th National Meeting of the A.I.Ch.E., April 1967.

7. Hulburt H.M. & Katz S., Chem. Eng. Science, 19, 555 (1964).

8. McCabe W.L. & Stevens R.P., Chem. Eng. Progress, 47, No. 4,168 (1951).

9. Miller P. & Saeman W.C., Chem. Eng. Progress, 43, No. 12, 667 (1947).

10. Murray D.C. & Larson M.A., A.I.Ch.E. Journal, 11, No. 4, 728 (1965).

11. Randolph A.D. & Larson M.A., A.I.Ch.E. Journal, 8, No. 5, 639 (1962).

12. Rumford F. & Bain J., Trans. Instn. Chem. Engrs., 38, 10 (1960).

13. Saeman.W.C., A.I.Ch.E. Journal, 2, No. 1, 107 (1956).

14. Shinnar R., Journal of Fluid Mechanics, Vol. 10, Part 2, 259-275 (1961).

15. Tanimoto A., Kobayashi K. & Fujita S., International Chem. Eng., 4, No. 1, 153 (1964).

16. Thomas & Mallison, Petroleum Refiner, No. 5, 211 (1961).

17. Van Hook, A., "Crystallization: Theory and Practice" ACS Monograph 152, p. 94, Reinhold, New York (1961).

18. Ibid., p. 13.

19. Worden & Amundson N.R., Chem. Eng. Science, 17, 725 (1962).

20. Robinson J.N. & Roberts J.E., Canadian Journal of Chem. Eng., 105, October 1957.

21. Bransom S.H. et al., Discussions Faraday Soc., 5, 83 (1949).

Autobiographical Statement

Martin B. Sherwin was born July 27, 1938 in New York City. He attended the City Public School System, graduating Lafayette High School in Brooklyn with an academic diploma in June 1955.

He then went to the City College of New York and received a Bachelor of Chemical Engineering degree in January, 1960.

Upon graduation, he went to work for the Scientific Design Company in New York as a process development engineer in the petrochemical area and continued his education on a part-time basis until September 1964. He attended the Polytechnic Institute of Brooklyn in the evenings, starting in January 1960, and received the Master of Science degree in Chemical Engineering in June 1963.

He started attending the City University as a part-time student in January 1963, after being informed that they would soon start a Doctoral program. In September 1964 he accepted a Lecturer's position in the Chemical Engineering Department of the City University.

The next two years were spent teaching in the undergraduate school and working toward a Ph.D. degree. He successfully defended his Ph.D. dissertation on November 30, 1966.

Upon completion of the requirements, he left the college to accept the position of Manager of Chemical Engineering Development at Chem Systems, in New York City.

MBS:bes